ROLE OF LONG-RANGE PROJECTING INHIBITORY NEURONS IN HIPPOCAMPAL NETWORK OSCILLATIONS

by

ALBERT DAVID TAMBURRI

A thesis submitted to the

University of Birmingham

for the degree of

MASTER OF PHILOSOPHY

Department of Physiology
Medical School
University of Birmingham

July 2012

ABSTRACT

In this study, I investigate the role that hippocampal inhibitory cells (interneurons) have on the synchronization of oscillations between the two hemispheres of the hippocampus. My study focuses in particular on the ripple oscillations, because this network activity is highly synchronous between left and right hippocampus.

My hypothesis is that a subset of hippocampal interneurons might establish axonal connections from the hippocampal area in which the somata reside towards the contralateral side, hence regulating inter-hippocampal ripple discharges. I address this hypothesis injecting in one side of the hippocampus substance P fragment, a peptide that increases the activity of subsets of inhibitory neurons in rat hippocampus, and the antimalarial Quinine whose roles as gap-junction blocker has been well established by numerous publications. Simultaneous recording from both hippocampi are thus compared to investigate whether ipsilateral injected drugs affect hippocampal ripple activity recorded contralaterally.

I found that ripple oscillations are indeed affected by injection of the abovementioned drugs: Quinine increases length and decreases Inter Ripple Interval (I.R.I.) in both injected and contralateral hippocampus; on the other hand, SP decreases the average amplitude of the ripple episode, but increases the duration of the ripple event. Most importantly, many of the perturbations observed were preserved between injected and contralateral hippocampus. Since the drugs I employed affect mainly inhibitory neurons, I propose that long-range projecting inhibitory neurons located in the injected hippocampus are responsible for carrying the drugs' effects to the contralateral hippocampus.

In conclusion, my results seem to indicate that long-range projecting interneurons are involved in transmitting ripple synchronization information across the two hippocampi.

TABLE OF CONTENTS

LIST OF ILLUSTRATIONS

INTRODUCTION

The hippocampus: anatomical overview

The hippocampus is a part of the brain located inside the temporal lobe; humans and other mammals have two hippocampi, one in each side of the brain. It forms a part of the limbic system (***Fig.1***) and plays a critical part in memory and spatial navigation; it is as well involved in neurogenic diseases such as Alzheimer's disease and epilepsy. For this reason, it is not surprising that nowadays this area of the brain is very much under the attention and scrutiny of many research groups throughout the world.

By the middle of the last century, the limbic system and especially the hippocampus have started to be one of the most investigated structures in the nervous system. It is from these early works that derives much of the current knowledge on how the hippocampus functions.

One of the most important body of works performed on the hippocampus has been carried out by Ramòn y Cajal in the late part of the 19th and early part of the 20th century. According to his works [1, 2], the hippocampus shows a peculiar cellular architecture, a very distinct laminar distribution, with layers containing almost exclusively cell somata and others that incorporate mainly dendrites, with little cell bodies to be found. In such architecture, neurons can be classified in either one of these two categories: "principal" and "non-principal" neurons, the latter ones known today as *Interneurons*. A more detailed characterization of non-principal cell types is found in the work of his pupil Lorente de Nò [3].

Although there is a lack of consensus relating to terms describing the hippocampus and the adjacent cortical region, the term hippocampal formation generally applies to the Dentate Gyrus, the Cornu Ammonis fields CA1-CA3, and the Subiculum [4] (***Fig.2A***). The CA1, CA2 and CA3 fields are often referred to as the hippocampus proper. Each of these areas show both the typical

neurons usually found in the hippocampus: *excitatory cells* that represent the majority of the neuronal population (~90%, i.e., principal cells) and *inhibitory neurons* (~10%, i.e. non-principal cells), which are much more diversified in terms of somata shape, position, dendritic and axonal arborisation and orientation, immunochemical content and electrophysiological properties [5].

Fig.1: Representation of the anatomical position of the Hippocampus inside the human brain (reproduced from the Boston University Science Magazine).

Much of our current knowledge about the neuronal organization of the hippocampal formation is mainly based on excitatory neurons studies, but the importance of inhibitory cells has started to be acknowledged. Their role in regulating the interaction among excitatory neurons (plasticity and synchronization) and their implications in network oscillations (theta, gamma, high frequency ripples) are examples of their crucial roles [5-9].

To sum up the information mentioned above: the hippocampus has two different sets of neurons, the *excitatory* ones (principal neurons), which form a trisynaptic pathway across the entire hippocampus (entorhinal cortex → dentate gyrus → CA3 → CA1) and are responsible for

most of its properties and roles (***Fig.2B***); the *inhibitory* ones (non-principal neurons, *Interneurons*) that regulate the firing pattern of principal cells [10].

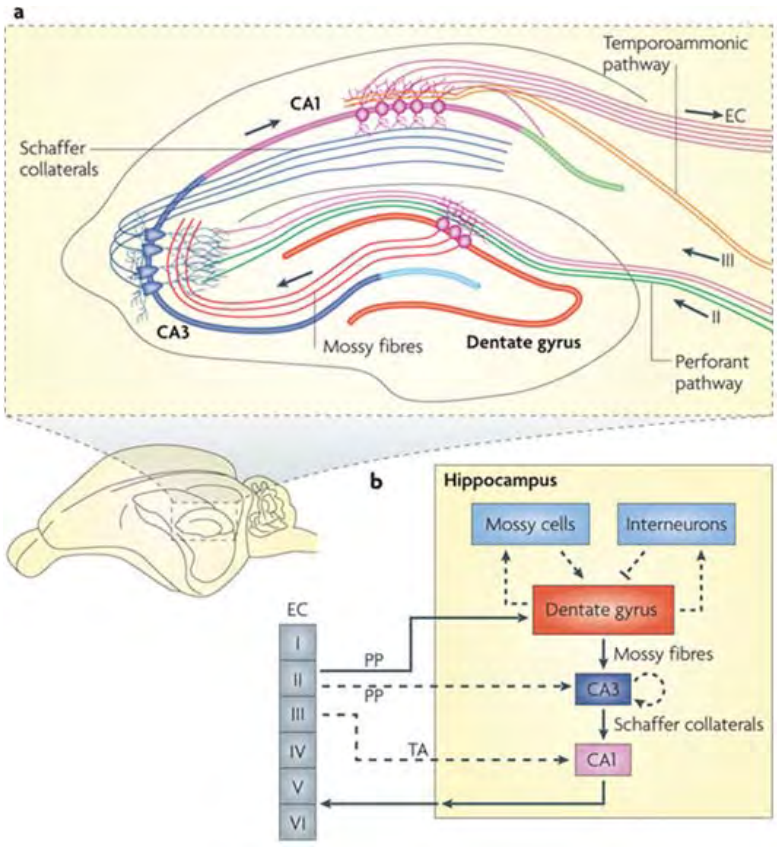

Fig.2A*:* An illustration of the hippocampal trisynaptic loop.
B: Diagram of the hippocampal neural network. The trisynaptic pathway (entorhinal cortex (EC)–dentate gyrus–CA3–CA1–EC) is depicted by solid arrows. The axons of layer II neurons in the entorhinal cortex project to the dentate gyrus through the perforant pathway (PP). The dentate gyrus sends projections to the pyramidal cells in CA3 through mossy fibres. CA3 pyramidal neurons relay the information to CA1 pyramidal neurons through Schaffer collaterals. CA1 pyramidal neurons send back-projections into deep-layer neurons of the EC. CA3 also receives direct projections from EC layer II neurons through the PP. CA1 receives direct input from EC layer III neurons through the temporoammonic pathway (TA). The dentate granule cells also project to the mossy cells in the hilus and hilar interneurons, which send excitatory and inhibitory projections, respectively, back to the granule cells (modified from [11]).

Network activity in the hippocampus

Neurons of the hippocampus produce different patterns of synchronized population activity supporting various phases of memory encoding, consolidation, and retrieval. These patterns are associated with different behaviours of the animal and serve to establish optimal conditions for

the dialog between hippocampus and neocortex [8, 12]. For example, when rats are actively exploring the environment, information from the neocortex is sent to the hippocampus via the entorhinal cortex [13] and this state is characterized by oscillations in the theta (4-9 Hz) and gamma (40-80 Hz) ranges (***Fig.3***). During consummatory behaviours and quiet awake periods, so called non-theta activity is interrupted by intermittent bursts of synchronized neuronal activity named sharp waves [14]. These sharp waves arise from the CA3 region and are transmitted via CA1 back to the entorhinal cortex [7]. The fine structure of these bursts includes fast oscillations at ~200 Hz, named ripples (***Fig.4***). Theta, gamma and sharp wave-ripple (SWR) activities also appear during REM sleep and slow wave sleep, respectively [7, 15-20]. The oscillatory context is imposed on the principal cells by networks of inhibitory neurons. Theta rhythmic input from the septum and from the entorhinal cortex is mediated by interneurons and involves feed-forward inhibition [21-23]. On the other hand, gamma and ripple oscillations in the hippocampus are believed to be generated locally by networks of inhibitory interneurons [24-26].

Although each oscillation is important for the normal activity of the brain, this work will focus primarily on sharp waves ripple (SWR) activity. For a review on the importance and characteristics of theta and gamma activity in the hippocampus, I therefore suggest the reading of these articles on the topic: [27-31].

The importance of ripple oscillations derives from the observation that during SWR time window, 50 to 100.000 neurons discharge synchronously in the CA3–CA1–subicular complex [14, 32]. Based on this observation, Buzsaki proposed that the SWR bursts are initiated by neurons whose recurrent connectivity had been transiently potentiated during the preceding awake experience of the animal [8]. Several later studies revealed that ensembles of neurons that fire together during a particular behavioural experience tend to ‘replay’ that experience during the following SWR episode [33, 34]. These cells fire together at high frequencies, which should promote Hebbian plasticity, i.e. Long Term Potentiation (LTP). In addition, as mentioned above,

the ‘content’ of the sharp wave events is determined by previous experience of the animal [33-36]. Because of the behaviour-relevant content and because of the three- to five-fold gain of network excitability during the SWR episode [14], this endogenous hippocampal output pattern is thought to play a critical role in transferring transient memories from the hippocampus to the neocortex for permanent storage [8].

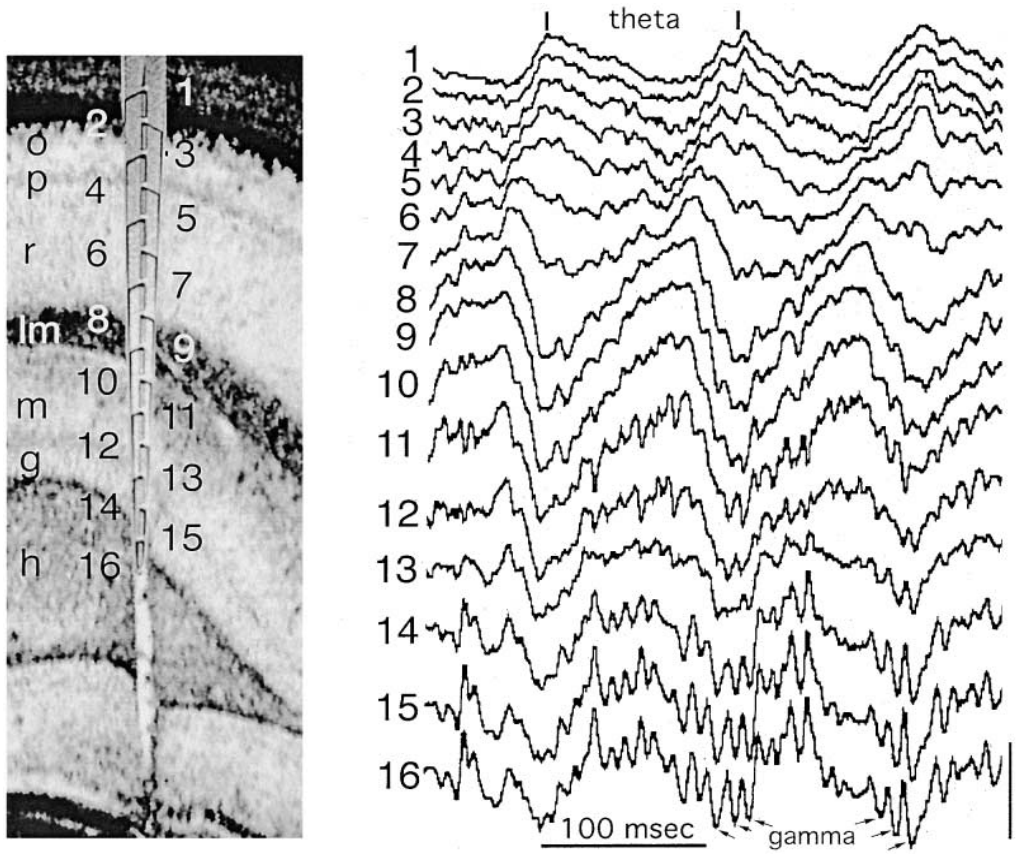

Fig.3: Voltage-versus-Depth Profile of Theta Oscillation in the Rat;
Left: a 16-site silicon probe in the CA1-dentate gyrus axis. Numbers indicate recording sites (100-μm spacing). Legend: o, str. oriens; p, pyramidal layer; r, str. radiatum; lm, str. lacunosum-moleculare; g, granule cell layer; h, hilus. Right: Theta waves recorded during exploration. Arrows mark gamma waves superimposed on theta oscillation. Vertical bar: 1 mV (modified from [37]).

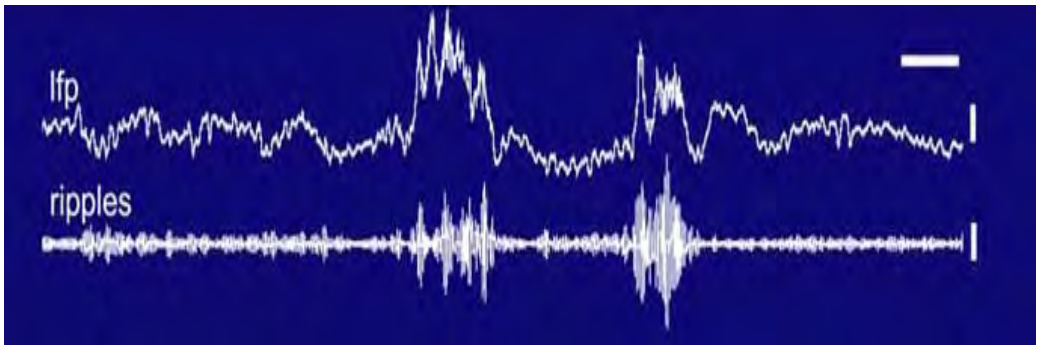

Fig. 4: Top trace: unfiltered local field potential (lfp) recorded in stratum pyramidale during ripple activity. Bottom trace: the same local field potential shown in the upper trace, filtered between 90 and 140 Hz, in order to show ripple activity. Calibration marks: top trace, 0.5 mV, 0.2 s; bottom trace, 0.1 mV (modified from [38]).

As other network oscillations (theta, non-theta), so too ripples between the two hippocampi are highly synchronized. Since theta activity is believed to be the result of the common input from the septal region [39], it is not surprising that the theta oscillation shows a high degree of synchronization between the two relatively distant hippocampi. What is surprising is that ripple activity, although lacking a common input from an external source, is also highly synchronous between the two hippocampi. This result suggests an important role of the commissural projections in inter-hemispheric network synchronization. Although current source density analysis [40, 41] revealed that oscillating pairs of sinks and sources during ripples were largely restricted to the pyramidal cell layer and its immediate vicinity, using partial coherence analysis it was demonstrated that the "coupling" between the two CA1 regions of hippocampi is stronger than between the individual layers of the same hippocampal hemisphere [42]. Excitatory axons connecting the two hippocampi have also been implicated in the ripple synchronization, but the very small time delay between the appearance of ripples (~1 ms) excludes any involvement of chemical synapses, which usually present a delay time of 2 to 5 ms [43]. Thus ripples seem to involve mainly electrical synapses, whose delay time is much shorter (~0.2 ms [43]). From these studies, it appears likely that synchronization between the hippocampal ripple activity is governed by inhibitory cells that connect both hippocampi together through means of their

chemical synapses. Nevertheless, the mechanism of the ripple synchronization remains uncertain.

Inhibitory neurons

Inhibitory neurons in the hippocampus use γ-amino butyric acid (GABA) as inhibitory neurotransmitter; they were originally considered as locally acting cells, thus the common name "local circuit neurons" is still in use, in spite of the fact that inhibitory neurons with long-range axonal arborisation have been described [44].

Inhibitory cells with axonal arborisation that is less than 1 mm in diameter can be considered local circuit neurons (i.e.: basket cell, chandelier cell, oriens cell with lacunosum-moleculare projection), whereas cells whose axonal arbour is larger than 1 mm belong to the long–range interneurons group (i.e. bistratified, trilaminar, back-projection cells [44]). The heterogeneity of inhibitory cells, bearing various morphological, neurochemical and electrophysiological properties ensures the proper function of the hippocampus. Therefore, it is believed that the spread of excitation in the hippocampus is controlled by the small number (~ 10% of the entire cell population) of inhibitory neurons. The various GABAergic inhibitory cell types are responsible for shaping behaviourally dependent network activities such as theta and sharp-wave associated ripple oscillation, coordinating principal cell discharge probability during complex network behaviors [45, 46].

Local circuit cells have been fairly well characterized using *in vitro* preparations. However, the study of long-range inhibitory cells, especially their role in network synchronization, requires *in vivo* approaches because of the truncated axonal arborisation that would occur *in vitro*.

Although already hypothesized in the past it was only recently demonstrated using the *in vivo* juxtacellular recording and labelling method that distinct subpopulation of inhibitory cells have different roles in various behaviourally dependent network oscillations [9, 47]. In most of

the mentioned experiments, mainly local circuit neurons were investigated [48]. However, information is still missing about how long-projections neurons participate in the hippocampal activity. It is hypothesized that long-range inhibitory cells exert a weaker, but more global effect on their target than local circuit inhibitory cells [44]. Hippocampal inhibitory cells with unusually long-range axonal arborisation have been reported in many recent works: one type is the Calbindin/Somatostatin immunoreactive hippocampo-septal neuron projecting into the medial septal region [49], the other known is the unique "back-projection" neuron located in the CA1 area sending dense axon collaterals to the CA3 and hilar regions (***Fig.5***; [44, 50]). More recently, it has been discovered that the two populations (hippocampo-septal and back-projection cell) are in fact the same [51].

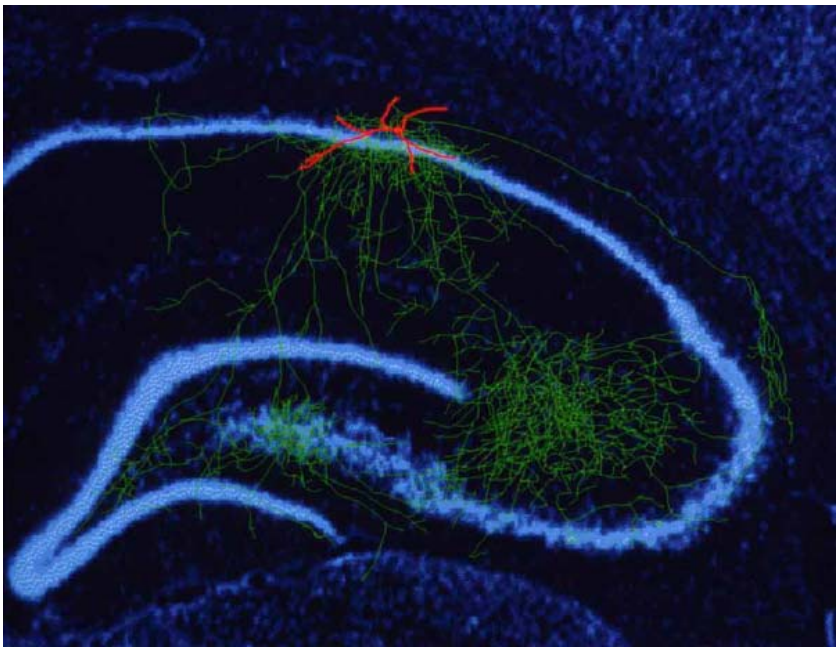

Fig. 5: Stratum Oriens long projection neuron: red: soma and dendrites; green: axonal arborisation. Notice the large axonal innervation this cell has within dentate gyrus, CA3 area and subiculum (from [44]).

The question then arises as to what is the role and impact of these long-range inhibitory cells in the function of the hippocampal neuronal network. A model has been proposed to explain the impact of long-range interneurons on hippocampal network oscillation [44, 50]. According to

this “master-slave” model illustrated below (***Fig.6***), in the hippocampus there is a local circuit neuronal population (i.e.: basket cells, axo-axonic cells, etc.) which truly acts locally (“slaves”), each neuron modulating the action of 1000-1500 excitatory cells.

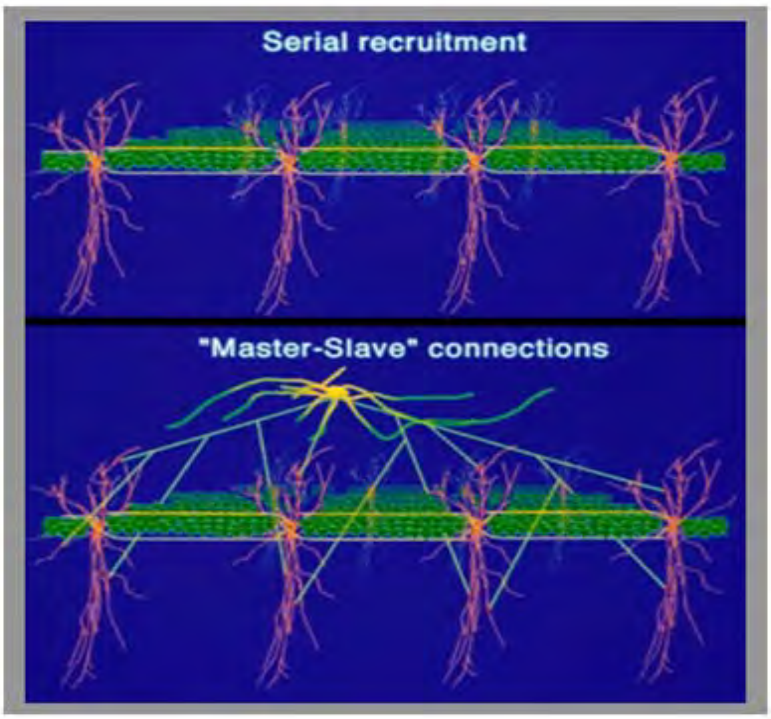

Fig.6: Master-slave model representation: in the upper panel, local circuit inhibitory neurons (basket cells in the illustration) are shown to innervate many pyramidal cells. In the bottom panel is shown that a single long projection neuron can innervate many hundreds of basket cells, therefore finely regulating inhibitory activity throughout the hippocampus (based on the findings published in [44] and [50]).

The upper layer of this model consists of the long-range inhibitory neurons (“masters”), which affect a much larger spatially dispersed population of excitatory neurons in two ways: one is a direct innervation of the excitatory cells (feed-forward or feed-back inhibitory mechanisms), the second is through modulating the actions of local circuit inhibitory neurons (disinhibitory mechanism). Obviously, the disinhibitory mechanism has a more global effect since the affected number of excitatory neurons is at least 1000-1500 times higher (thus tens of thousands of

neurons). This model can explain how the small number of inhibitory neurons is able to not only control the activity of excitatory neurons, but also precisely coordinate the network oscillation through the entire hippocampus. In order to validate further this model however, the neuro-anatomical (number, neurochemical contents, postsynaptic targets) and electrophysiological properties (firing properties, coordinating ability, etc.) of long-projection inhibitory neurons need to be investigated in future studies.

Ripples can be detected at the same time in areas spatially quite distant from each other: in particular, Buzsáki and colleagues showed that ripples can be detected from points that are at least 2 mm along the CA1 axis, with virtually no delay [7, 24]. The same group later showed that some cycles of the oscillations can be coherent over distances as long as 5 mm in the rat [32] and thus recruit the largest part of the whole CA1 region of one hippocampal hemisphere. Such a spatial extension rules out that ripples reflect bursts of single neurons and proves that a multicellular network is in place in order to generate, synchronize and maintain the ripple activity throughout the hippocampus. In addition, the coherence over large distances poses specific demands on the performance of the network. Although ripple activity can be detected in the CA1 pyramidal cells layer and its immediate surroundings, we know today that the origin of this oscillation resides in the CA3 area. As a matter of fact, ripples arise from CA3 pyramidal cells that, through their positive excitatory feedback loop, develop spontaneous, synchronous bursts of action potentials that then propagate to CA1 [7]. As mentioned earlier, CA3 pyramidal cells innervate the CA1 pyramidal cells of the same hippocampus, as well as the CA3 pyramidal cells of the contralateral hippocampus [52]. Moreover, because of the short time delay between the simultaneously recorded ripples (1-1.5 ms) it is unlikely that multisynaptic pathways are involved. As a matter of fact, axonal conduction velocity in the hippocampus is less than 1 m/s [53]; thus, for an action potential it takes at least 5 ms to travel 5 mm (which is the average distance between left and right hippocampus, in rodents), not considering the delay time

between chemical synapses. Therefore, to generate a sequence of simultaneous action potentials with intervals of 5-10 ms (as during ripples) over such large distances, neurons must be coordinated by a faster mechanism than mutual exchange of action potentials. It has therefore been suggested that gap junction signaling might be involved in the synchronization of ripples [54-56].

Gap junction and their involvement in hippocampal activity

The idea that electrical signaling via gap junctions may be involved in synchronizing neuronal activity in the mammalian brain is far from new. A role for gap junctions in the synchronization of neuronal activity has already been proposed by a number of authors, in particular concerning the hippocampal pyramidal cells [57-59]. Recent studies both *in vivo* and *in vitro* have also revealed that electrical signalling between homogeneous populations of neurons might be involved in generating the typical hippocampal rhythmic, synchronous population activity, such as gamma frequency oscillations [60-63] and ripples [7, 64]. Coupling was initially demonstrated between principal (pyramidal) cells [57-59] but this is currently highly debated. Interneurons however undoubtedly form electrical synapses as was demonstrated electrophysiologically and morphologically using electron microscopy [65-67].

Gap junctions are formed by proteins called connexins (Cxs) that are expressed in most tissues of the body. Although several gap junction proteins are expressed in the Central Nervous System, Cx36 has been shown to be preferentially, if not exclusively, expressed in neurons [68, 69]. *In situ* hybridization studies in the adult mice showed that Cx36 expression was largely absent from the pyramidal cell layer, with labelling occurring in *stratum oriens* and *radiatum*. Single-cell PCR showed that Cx36 is expressed in different types of GABAergic interneurons [70]. This pattern of localization suggested that the majority of neurons expressing Cx36 are likely to be GABAergic interneurons. Experiments using the Cx36 knock-out mice confirmed

this hypothesis since gamma oscillations were significantly smaller than those recorded in the wild-type mice [71, 72]. Despite the strength of gamma frequency oscillation was significantly affected in the hippocampus of the Cx36 KO mice, fast ripple oscillations in this region were largely unchanged when compared to wild-type mice [73]. This result is not surprising, since gamma oscillations are thought to be synchronized by local circuit neurons. What is surprising is that ripple oscillations were maintained in Cx36 KO mice, irrespective of the loss of a major neuronal connexin. One of the reasons why the authors were not able to detect any changes in the ripple activity between WT and KO mice might reside in the *in vitro* technique employed during the experiments. Such a technique employs brain slices of various thickness: in such a condition, long-projection neurons would suffer a major impairment to their synchronizing power because most of their contralateral axons are cut away during the preparation of the slice.

Substance P and influence on the activity of long-projecting interneurons

Substance P (SP), along with neurokinin A and B, is a tachikynin family peptide that acts as a neurotransmitter or neuromodulator. It is widely distributed in the central and peripheral nervous system [74] where, similarly to other tachikynins, it is believed to be important in pain perception [75] and to promote vasodilatation [76]. The biological actions of the tachikynins are mediated through three kinds of receptors, NK-1, NK-2 and NK-3 [77]. In the hippocampus, the amount of NK-1 mRNA was found to be two orders of magnitude higher than NK-3 [78], while the density of NK-2 binding sites was reported to be even weaker than that of NK-3 [79]. This demonstrates that the NK-1 receptor is the most abundant tachikynin receptor in the hippocampus. SP exerts its actions mainly through activation of the NK-1 receptor [80]. Neurons immunoreactive for this receptor were identified in the dentate gyrus, strata oriens and pyramidale of the CA1 and CA3 areas [5, 81]. Nonetheless, an old intracellular study found no direct effect of SP on pyramidal neurons of the CA1 area [82], which is not surprising

considering that pyramidal cells do not express SP receptors [5] and only interneurons do [83]. An excitatory action of SP on presumably non-pyramidal cells was instead found by Dreifuss and Raggenbass [84] using extracellular recordings. This study prompted Kouznetsova and Nistri to investigate whether SP can modulate inhibitory neurons' synaptic transmission in the hippocampus. The results of this *in vitro* study suggest that SP is able to induce depression of fields potentials recorded from stratum pyramidale [85]. The two researchers also found that SP is able to increase the frequency of spontaneous GABAergic events and reduce that of spontaneous glutamatergic events, but no change in amplitude was observed [85, 86]. These effects would produce a change in gain setting of the inhibitory network, which could potentially affect the output of pyramidal neurons. The researchers finally proposed stratum oriens interneurons expressing NK-1 receptors as responsible for mediating SP effects on the hippocampal network. This notion is interesting considering that it was suggested that oriens GABAergic interneurons act as "gatekeepers" of CA1 pyramidal cell activity [87].

In spite of the information above, the role of SP in the hippocampus remains uncertain, even more so considering that there is a localization mismatch between endogenous SP and its receptors [83], in agreement with the hypothesis that the peptide acts at a substantial distance from the site of its release [88]. Nonetheless, since in recent years it was proposed that the peptide can facilitate learning in the rat [89, 90], I decided after consulting with my supervisor to include SP in my project. This was done to investigate if and how the peptide exerts its actions via modulation of ripple activity in the hippocampus. If SP were indeed able to act positively on long-projecting stratum oriens interneurons, I would expect it to promote a disinhibitory effect on CA1 pyramidal neurons, which might in turn result in an increase of ripple activity in the injected side as well as in the contralateral side.

Research hypothesis and experimental approach

Since data is missing about the extent and strength these long-projection cells have upon the synchronization of ripples, I performed *in vivo* recordings of ripple activity before and after injection of the gap-junction blocker Quinine and the neuroactive peptide SP. The aim of this work is therefore to investigate what is the influence of such long range projecting cells on the synchronization between the two hippocampi concerning ripple activity. Since the juxtacellular or intracellular labelling of such cells is technically very challenging due to the small number of long projection neurons in the hippocampus, I relied on an indirect approach.

Based on the assumption that such long projection cells innervate mainly inhibitory neurons in both sides of the hippocampus, I tested whether the interference of communication between inhibitory cells in one side of the hippocampus through selective gap-junction blocking agents had a discernible effect on the contralateral side. In order to modify the communication between the inhibitory cells' network, I injected in one side of the hippocampus (hence forth termed ipsilateral side) drugs that are known to act as Cx36 gap-junction blockers (Quinine [91, 92]) as well a drug that has been shown to specifically increase inhibitory neurons' activity in the hippocampus (SP fragment [89, 93]). My hypothesis is that if ripple oscillations between the two hippocampi are modulated by long projection cells, I should be able to detect a change in various parameters (synchronization, signal delay, amplitude and frequency) of the ripple oscillation in the side of the hippocampus that has not been injected with the drug (from now on referred to as contralateral side).

I therefore suggest that the synchronization of ripple activity between the two hippocampi is at least in part modulated by the actions of a particular subset of inhibitory neurons that project to both sides of the hippocampi, being therefore able to synchronize the activity of a large number of neurons.

MATERIALS AND METHODS

Animal preparation

Sprague-Dawley male and female rats (250 to 400 grams) were used in this study. Any influence that the gender of the animal might have on ripple activity was not considered in the present study and should be addressed in future works. Animals were housed by groups of 1-2 in controlled ambient temperature polycarbonate cages with *ad libitum* access to food and tap water and maintained under a 12:12 light-dark cycle. All experimental procedures were performed in accordance to the guidelines provided by the Canadian Council on Animal Care (for experiments that were performed in Canada) and the Animals (Scientific Procedures) Act 1986 and associated regulations under approved project and personal licences (for experiments that were performed in the UK). Procedures were performed in accordance to Laval University Committee on Ethics and Animal Research and by the University of Birmingham Home Office Committee. Experiments were conducted at the Université Laval in Quebec City, with follow-up experiments performed at the University of Birmingham. Detection of ripple events was performed online and offline at the University of Birmingham; further analyses, including analysis of the parameters of ripple activity reported below, were performed using a MatLab program developed in collaboration with Professor Tiersinga's research group (Department of Physics and Astronomy, University of North Carolina at Chapel Hill, NC).

Rats were anaesthetized using urethane, a non-reversible anaesthetic (1.25 g/kg of body weight) in concomitance to supplementary doses of either Ketamine/Xylazine (87:13; 0.1-0.4 ml injected) or Ketamine/Metedomidine cocktail (7:3; 0.1-0.2 ml injected) to maintain a sustainable level of anaesthesia throughout the experiment. Body temperature was monitored through the use of an anal probe and maintained with a heating pad at 37° Celsius. Anaesthesia level was monitored every 30 minutes through a light pinch of the tail or the hind paw of the animal: if the

animal showed any signs of withdrawal reflexes, an additional 0.1 ml of Ketamine/Xylazine cocktail was administered. Also, changes in the recorded EEG of the animal from a non-theta to a sustained (non-transient) theta activity, signalled the possibility that the level of anaesthesia was decreasing. The head of the animals was fixed in a stereotaxic apparatus and an incision was made on the scalp to uncover the skull. Two holes were drilled above each hippocampal formation (AP: -3.6mm, ML: ±2mm, [94]). One hole was drilled on the left side of the skull to allow drugs and saline injections to the CA1 area of one hippocampus (AP: -5.9 mm, ML: -4.3 mm, [94]). To this avail, a special 45°/45° angle manipulator was employed to deliver drugs and control solutions in the contralateral hippocampus. Drugs and control solutions were this way injected always in the left hippocampus, in order to standardize the protocol followed. Two additional small holes were drilled above the frontal cortex for inserting the probes' reference electrodes. Also, a ground electrode was inserted under the skin of the animal.

Recording equipment

The extracellular field potential was recorded with 16- or 32- electrodes (Neuronexus) silicon probes. A multichannel recording device (Tucker-Davies Technologies) amplified the recorded signal. I implanted one probe in each of the hippocampi of the animal, using the same kind of probe for both hemispheres, which is to say that when a 16 electrodes probe was used in the right hippocampus, an identical 16 electrodes probe would be used for the left hippocampus too. This was done in order to have the same depth profile in both hemispheres and to rule out possible artifacts given by the probes' different positioning.

The probes (***Fig.7***) have a 10 mm silicon tip that could be easily inserted in the neuronal tissue. Each probe has a variable number of recording electrodes (16 or 32), according to the model employed. Both types of probes have been employed in this study: in particular, I used the 16 electrodes probes in 4 experiments, employing the 32-electrode probes in the remaining 12

experiments. The 16-electrode probes (Neuronexus model A1X16, ***Fig.7A***) had 16 recording sites on one single silicone shank. In this kind of probe, recording electrodes are spaced 100 μm from each other, for a total length of the probe of 3.0 mm; the recording area of each electrode is about 154 μm^2. This probe allowed us to record depth profiles of the activity in the hippocampus from stratum Oriens to the lower blade of stratum Moleculare, with little overlapping activity between adjacent layers, given the small area each electrode had. On the other hand, the 32-electrode probes (Neuronexus model A4x8, ***Fig.7B***) were built by four silicon shanks, with a spacing of 500 μm between shanks. On each shank, 8 electrodes resided, each spaced 200 μm from one another. Even in this case, the area of the electrodes was about 154 μm^2.

The particular way this model is built allowed us to monitor and record oscillations in the hippocampus over a 2 mm horizontal section, even in this case from stratum Oriens to the lower blade of stratum Moleculare. Although the quality of the recordings was the same independent of the kind of silicon probes used, the preference for using the 32-electrode probes has been made based on the observation that the 16-electrodes probes were found to be much more fragile than their more resistant, 32-electrodes counterpart. This is because the bulkier, four shanks 32-electrode probe (***Fig.7B***) is able to distribute the pressure applied by the tissue on the probe in a more balanced fashion compared with their slimmer, 1 shank, 16-electrodes counterpart (***Fig.7A***). The probes were at first lowered by 2.0 mm from the surface of the cortex, so that the very tip of the probe would sit just above the hippocampus. Then they would be moved slowly further down until clear unit activity from the CA1 pyramidal cells could be observed. Presence of SWR was another indication that the electrodes were in the correct position.

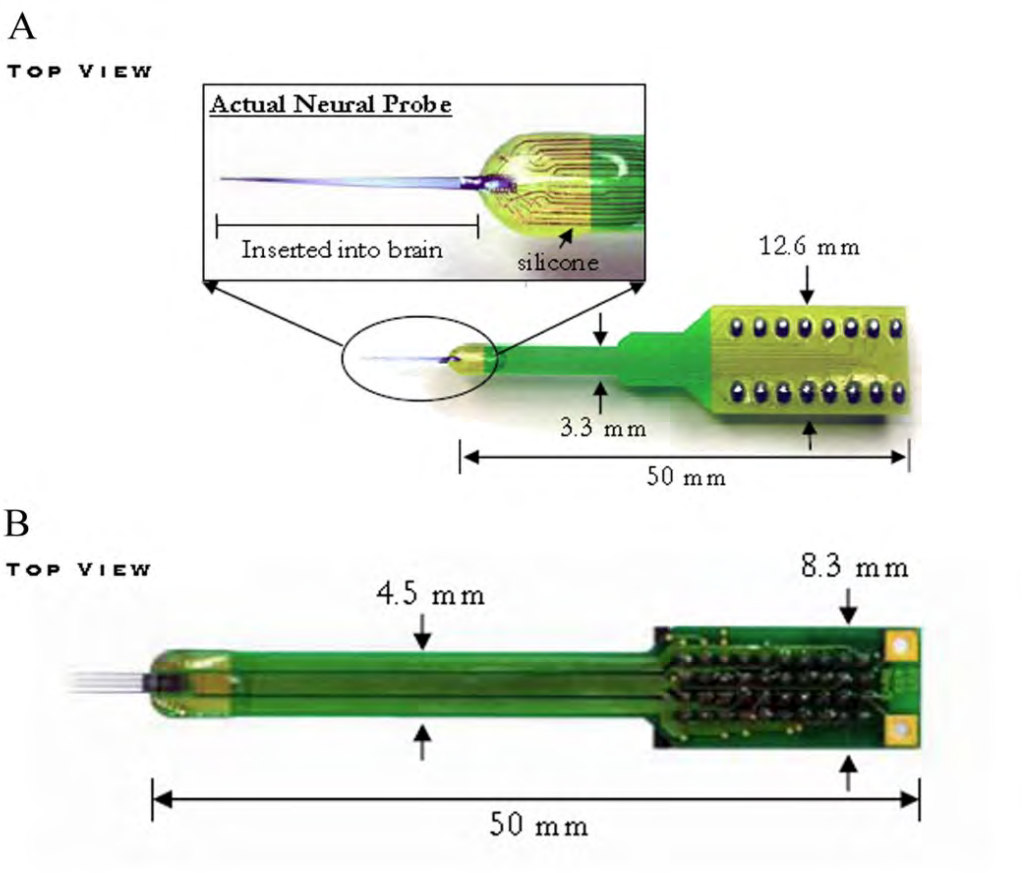

Fig.7A: 16-electrodes multichannel recording probe. The electrodes were built in one single row, with the 16th being the deepest electrode and the first being at the top of the probe. ***B***: 32-electrodes multichannel recording probe: in this case, each shank holds 8 recording sites, number 8 being the deepest one inserted in the tissue and number 1 being the topmost one (from Neuronexus, Inc.).

The extracellular field activity recorded through the silicon probes described above (sampling rate 3 KHz) was displayed using the Open Ex software (TDT Technologies); a selection of six to eight channels from both left and right probes was then made and displayed on Chart 5.0 software (AD Instruments). Of this selection, one channel from each hemisphere displayed on Chart was on-line band-pass filtered between 3 and 8 Hz in order to monitor theta activity, while the remaining channels were filtered between 80 and 200Hz, allowing the operator to monitor in real-time hippocampal ripple activity. Channels recorded with the TDT software were instead stored unfiltered for off-line data analysis.

The position of the probes was traced using the red lipophilic fluorescent Dioctadecyl Indocarbocyanine dye (DiI from Molecular Probes; 1% in DMSO). Simply put, at the beginning of each experiment the tip of both probes was manually dipped into a small 0.5 μl transparent Eppendorf containing the DiI dye solution. Since the silicon probes are extremely fragile, this operation requires a very firm hand in order not to break the probes. Once the electrodes had been dipped into the dye solution, they were mounted on micromanipulators and lowered into the hippocampus, according to the procedures described above.

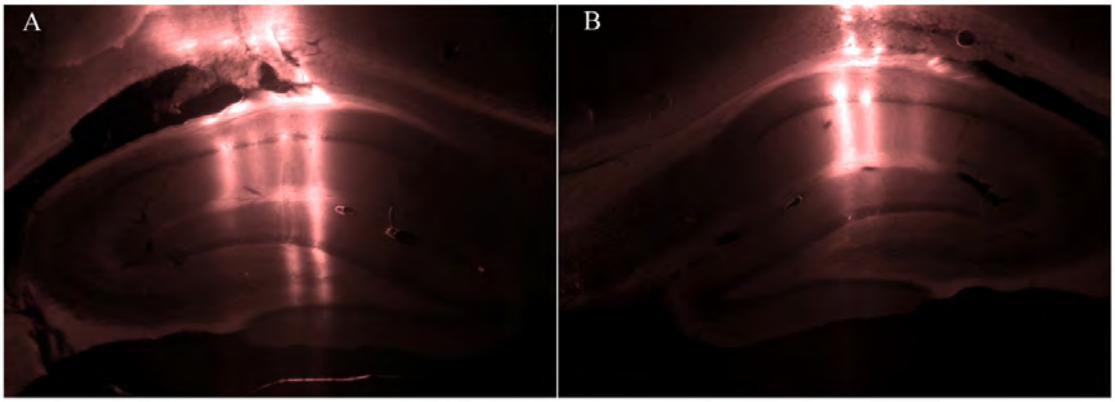

Fig.8: Traces of the 32-electrodes probe employed in this study; ***A***: contralateral side: notice the bright trance of all the 4 shanks that cross the entire length of the hippocampus. Only channels recording from the pyramidal cells layer were considered in the data analysis process. ***B***: ipsilateral side: two shanks of the 32-electrodes probe are clearly visible. The other two were found in the section cut immediately after the one presented in the figure.

Chemicals

Control injection site was marked through concomitant injection of the tracer Neurobiotin (2% in 0.9% in saline solution, Vecta). Glass graduated micropipettes (0.5-1 μm, resistance 1-2 MΩ; maximum capacity: 10 μl) were used to deliver the tracer and the drugs into the cerebral tissue. Neurobiotin was later developed in conjugation with the secondary antibody Marina Blue, so that the injection site would be labelled in a different colour than the probes' (DiI, red; Marina Blue, blue). Following control solution injection, the activity of the animal's brain was recorded for a 20-30 minutes period. This recording would later be compared to recordings under drug

conditions. A recovery period of at least 15 minutes was then allowed to the animal, after which drugs were delivered and the activity in the brain of the animal was again recorded for 20 to 30 minutes. The length of the recordings varied according to the ripple activity showed by the animal: poor ripple activity required longer recordings.

Drugs utilized in the experiments were SP fragment (1 μl, 5 nM; Sigma, Germany; n=7 animals) and Quinine Sulphate (1 μl, 30 and 300 μM; Sigma, Germany; n=7 animals). All solutions were dissolved in saline 0.9%. All drugs and control solutions were injected at a rate of 0.2 μl/s (taking about 5 seconds to complete the injection of a 1 μl solution). Drugs were kept at room temperature for 30 minutes before the injection, in order to rule out any temperature-related effects.

Completion of the experiment and recovery of the brain

As the experiment ended, animals were intracardiacally perfused with 4% paraformaldehyde in PB 0.1M, pH 7.4, the brains removed and cut with the use of a Leica Vibratome (50 to 70 μm-thick slices) and the electrode position was verified (***Fig.8***). Pictures of the position of the probes were taken, in order to select specific channels that would undergo data analysis. Only animals whose implanted probes were found in the hippocampus have been considered for the data analysis process. Furthermore, of the probes whose final destination was the hippocampus, only those channels that recorded from the CA1 pyramidal cell layer or its immediate surroundings were considered in the data analysis process. The selection of such channels was based on the images of the probes as well as the size of the ripples activity recorded during the experiments.

Immunohistochemical protocol

In order to verify that drugs and control solution was successfully delivered to the left hemisphere of the hippocampus of the animal, the control solution was added with Neurobiotin

2% (see above). Slices from the injected side of the brain were later washed with a phosphate (PB 0.1M) and Tris (TBS 0.05M, pH 7.4) buffers for 5 to 10 minutes. Sections were then blocked with normal goat serum (NGS 5%) in TBS for 30 minutes. The blocking solution was also added of the detergent Triton 100-X (0.5%), in order to increase antibody penetration. Following 3 additional washes with TBS (5 to 10 minutes each), sections were treated with the Streptavidin-Marina Blue (1:500, Molecular Probes) fluorophore complex, in order to visualize Neurobiotin in the stained tissue. Sections were then analyzed through fluorescence microscopy (Olympus AX70) Unfortunately, the little photo-stability of the Marina Blue antibody, along with the extremely bright fluorescence given by the DiI dye, prevented us from obtaining clear pictures of the injected sites. Nonetheless, only experiments in which visual confirmation of the injected site was unequivocally confirmed by comparison with the surrounding hippocampal anatomy were deemed successful and included in the results.

Data analysis

As mentioned above, detection of ripple events was performed online during each experiment. Offline analyses were required to identify a selection of channels that would undergo further analyses. Analysis of the parameters of ripple activity reported below was performed using a program designed in MatLab in conjunction with a collaborating laboratory (Prof. Tiersinga's research group, Department of Physics and Astronomy, University of North Carolina at Chapel Hill, NC). The program was developed by the collaborating laboratory, and tested for ripple detection using recordings provided by me and my laboratory. Once the MatLab program was appropriately tuned as to properly discriminate between ripple events and non-ripple activity (including artifacts), it was used by me to identify ripple episodes and provide maximal amplitude, frequency, length for each episode and the time between two succeeding episodes. The software scanned the recordings of each animal in every given condition (control

and drug injection) and discriminated between ripple and non-ripple events (theta and gamma activity, artifacts) based on a triple cut-off:

1) Ripple episodes had to last 50-150 ms: artefacts have smaller lengths while longer episodes in the same frequency might be regarded as epileptiform activity or other non-physiological conditions;

2) the frequency of the event had to be comprised between 80 and 200 Hz: this cut-off is generally accepted as the ripple window frequency;

3) the amplitude of the ripple event (in Volts) had to be sufficiently big (>3.5 SD) in order to be easily and immediately discriminated from background activity: this cut-off allowed us to discriminate between high frequency gamma oscillations (80 Hz) and low-frequency ripples, keeping the latter for analysis while discarding the former.

Channel selection process

In this work, given the same time window for recordings under control conditions and following drug injection (10 minutes), I investigated various parameters related to ripple activity. These parameters included number of ripple episodes, length, amplitude and frequency of each episode as well as the Inter Ripple Interval (I.R.I.), which is to say the time elapsed between two consecutive ripple episodes. All parameters were detected through the use of the MatLab software described above. One of the cut-offs for identification of ripple events is that the power of ripples (in mV) had to be above 3.5 SD from background noise in order to be detected as a ripple and hence included in the results. On the other hand, it could be argued that the amplitude of the ripple events varies in relation to the proximity of the recording electrode. For this reason, in comparing the amplitude of ripple events recorded from both hippocampi, one must be careful to compare ripples recorded from the same area, to avoid drawing erroneous conclusions.

In fact, when recording hippocampal activity using multi-electrode probes (***Fig.7A*** and ***B***), I usually observed ripple events from most of the electrodes placed in the hippocampus. Ripple

activity was observed to be strongest in the pyramidal layer [95] and indeed the amplitude of the events recorded varied according to the distance between recording electrode and pyramidal layer (for an example, see ***Fig.9***): the farther away from the pyramidal layer, the weaker the ripple appeared.

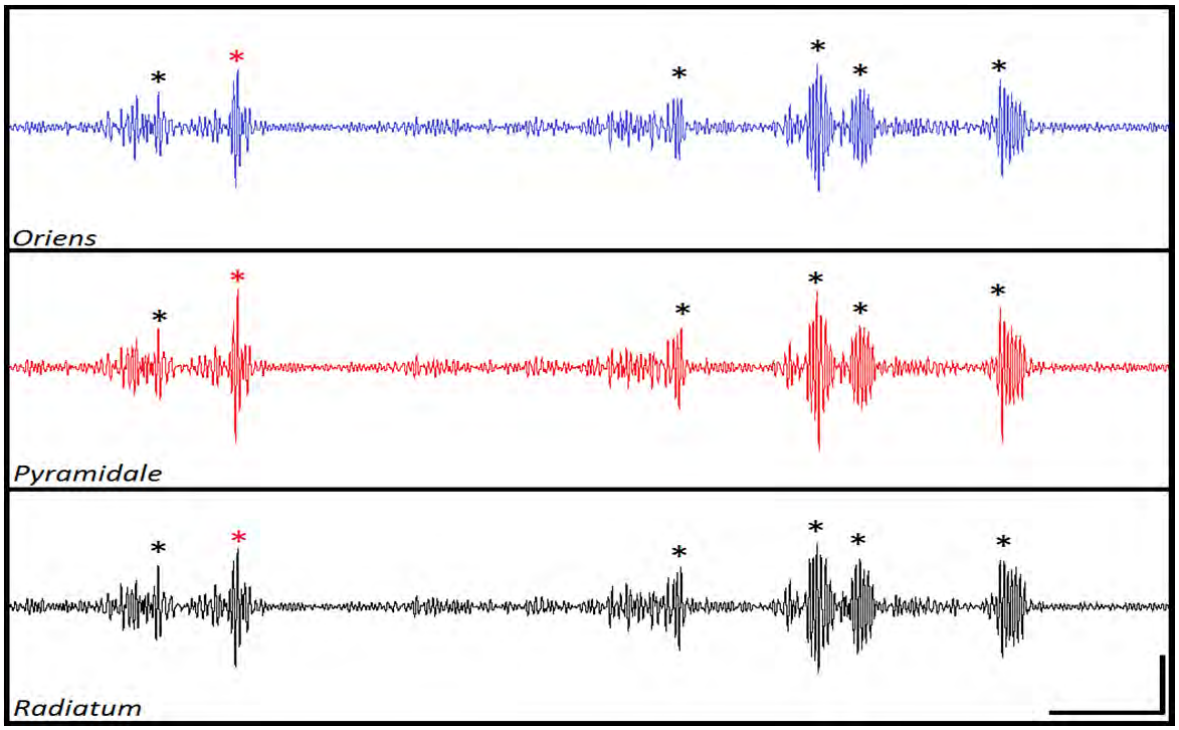

Fig.9: Amplitude of ripple episodes recorded from consecutive electrodes. The figure shows local field potentials from three consecutive electrodes, recorded under control conditions and filtered between 80 and 200 Hz in order to show ripple activity. The middle trace (red) shows the strongest deflection from background activity in terms of amplitude and was assumed to be recorded by an electrode positioned in the pyramidal layer. The traces immediately above (blue) and below (black) this putative pyramidal trace show ripple activity having comparable, although slightly smaller deflections from background activity. For this reason, I assumed that electrodes positioned in the *strata oriens* and *radiatum* respectively recorded the traces. As an example, the ripple marked with a red asterisk was found to have amplitude of 1.95 mV in *stratum oriens*, 2.27 mV in *stratum pyramidale* and 2.06 mV in *stratum radiatum*. Asterisks mark when ripple events occurred. Red asterisk marks the ripple event used in the example above. Calibration marks: horizontal: 0.2s; vertical: 1 mV.

Seeing as a visual evaluation of the electrodes positioning is impossible to do *in vivo*, because of the minute size of the electrodes (154 μm^2, see ***Fig.7***) and because the probes were removed prior to the recovery of the animals' brain, I had to rely on an indirect approach to trace back which electrode recorded activity from the pyramidal layer.

Given that the average height of the pyramidal cell layer in rodents is about 30-50 µm, I assumed that at least one of the electrodes used would have recorded activity from this layer. Based on this assumption, I compared the traces recorded from all the electrodes and screened for the amplitude of the events. I then selected the channel in which ripple activity was the strongest in terms of deflection from the background and assumed this electrode to have recorded from the pyramidal layer. This was also indicated by the fact that I was usually able to observe smaller ripple events (in terms of amplitude) in the channels immediately above and below the selected one (layers Oriens and Radiatum, respectively as reported in ***Fig.9***). This channel, which was assumed to have recorded from the pyramidal layer, underwent further analyses to explore all the parameters investigated in this study.

Statistical tests

Student's and Kolmogorov-Smirnov tests were used in order to determine the statistical relevance of analysed data. Data were deemed to be statistically relevant if the t-test between control and drug conditions showed a $p<0.05$; the t-test was paired, since traces recorded under drug injection were compared to recordings taken from the same animal prior to drug injection. In order to evaluate relevance for population distributions, I performed a two-sample Kolmogorov-Smirnov (KS) test on given data. The tool used to perform KS test was developed by the department of Physics at the College of Saint Benedict & Saint John's University (MN, USA) and can be accessed online through http://www.physics.csbsju.edu/stats/KS-test.html. Data is presented as mean ± Standard Deviation (SD).

RESULTS

General overview

Ripple activity across the hippocampus is highly synchronized. The onset of ripples event can be seen while recording from both sides of the brain, with a delay close to one millisecond. In the experiments, simultaneous recordings from both hippocampi (CA1, stratum pyramidale) were performed. As expected, oscillation at theta frequency was highly synchronous. During non-theta activity, ripple events emerged simultaneously in both hippocampi. Considering all the experiments performed, the ripple activity lasted from a few seconds to over 5 minutes, often interrupted by periods of theta activity of variable length or by periods of non-theta activity in which no noticeable ripple event were recorded. When the animal entered a period of intense ripple activity, the oscillations were detected in all the layers from which the probes resided, even several μm away from stratum pyramidale. Ripple episodes appeared spontaneously and were usually accompanied by a noticeable deflection in the otherwise regular non-theta rhythm. Although not as commonly, sometimes I also recorded ripple activity between periods of theta activity; this means that during theta activity a time window of several seconds could appear in which ripple activity was predominant; following this period, the animal would often go back to theta activity. A similar behaviour has already been reported by Csicsvari's group [96]. An excerpt of unfiltered as well as filtered traces recorded during one of the experiments is shown in the next page (***Fig.10***). As shown in the figure, analysis of the filtered ripples showed high synchrony between the two hippocampi (boxed section in ***Fig.10 B***, magnified in ***C***).

In order to investigate whether the gap-junction blocker Quinine [92, 97, 98] and the neuroactive peptide Substance P [99] affect the hippocampal ripple activity acting on subsets of inhibitory neurons, I monitored various parameters of the ripple oscillation and compared them to the ones recorded under injection of saline (control solution).

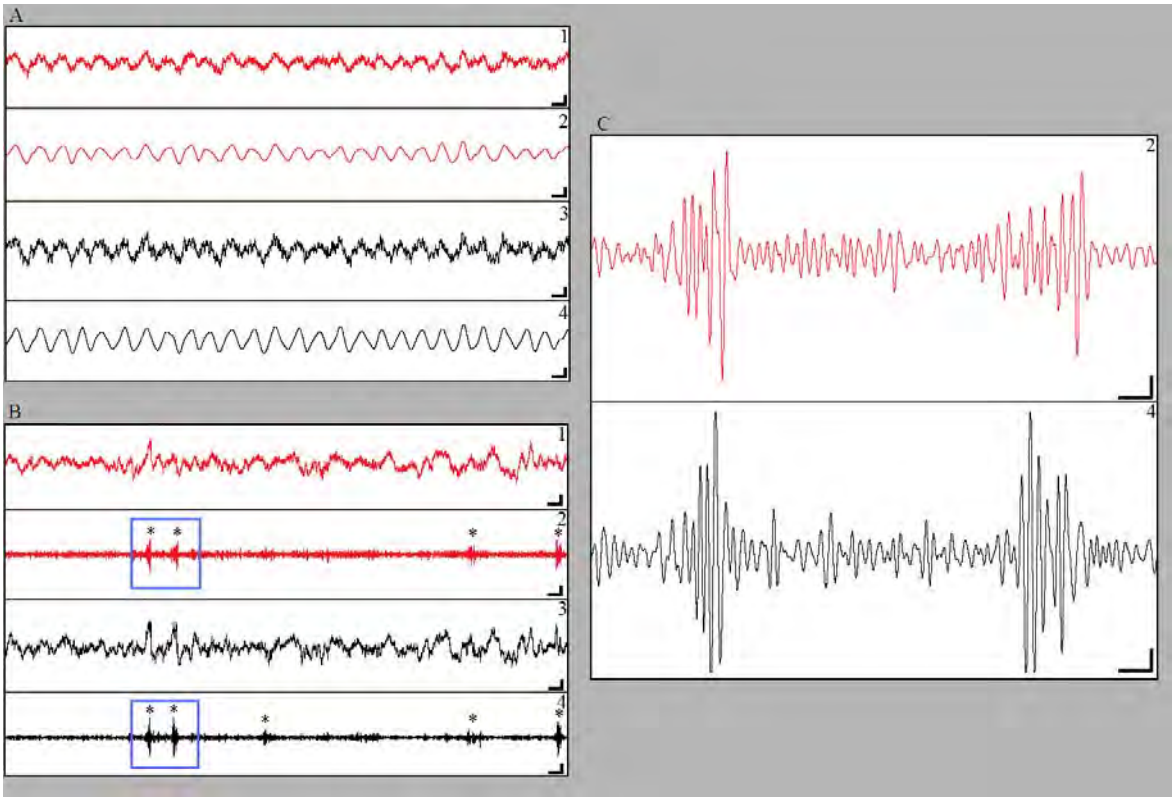

Fig.10 A: Local field potential showing theta activity recorded from stratum pyramidale. Red traces represent recordings from the injected side (left hippocampus) upon injection of the control solution, while the black traces are from the contralateral side (right hippocampus). Traces 1 and 3 are unfiltered, while traces 2 and 4 were filtered between 3 and 8 Hz in order to better show the theta activity. Calibration marks, horizontal: 0.2 s; vertical 0.2 mV; ***B***: Local field potential recorded from the same site as in ***A***, in this case showing non-theta and ripple activity; as above, red traces are recordings from the injected side (left hippocampus) while the black traces are from the contralateral side (right hippocampus). Traces 1 and 3 are unfiltered, while races 2 and 4 were filtered between 80 and 200 Hz in order to show ripple events. Asterisks indicate when ripple events occurred. Calibration marks: horizontal: 0.2 s; vertical 0.2 mV; ***C***: magnification of the boxed selection in ***B***, showing two strong ripples concomitantly recorded in both the right (red, trace 2) and left (black, trace 4) hippocampus. Calibration marks, horizontal: 0.2 s; vertical: 0.2 mV.

Quinine

The first parameter considered in this study is the number of ripple episodes recorded upon injection of a control solution as opposed to injection of Quinine in the two concentrations used. To do so, I compiled the number of ripples detected in a random 10 minutes time window in control condition and after drugs injection. In the seven experiments performed, I recorded on average 298.8 ± 26.1 ripple episodes in the injected side for the control period; this number

decreased to 143.3 ± 25.3 and 140.6 ± 28.4 following Quinine injection (30 and 300 μM, respectively), a decrease to 48 and 47% of the control, respectively.

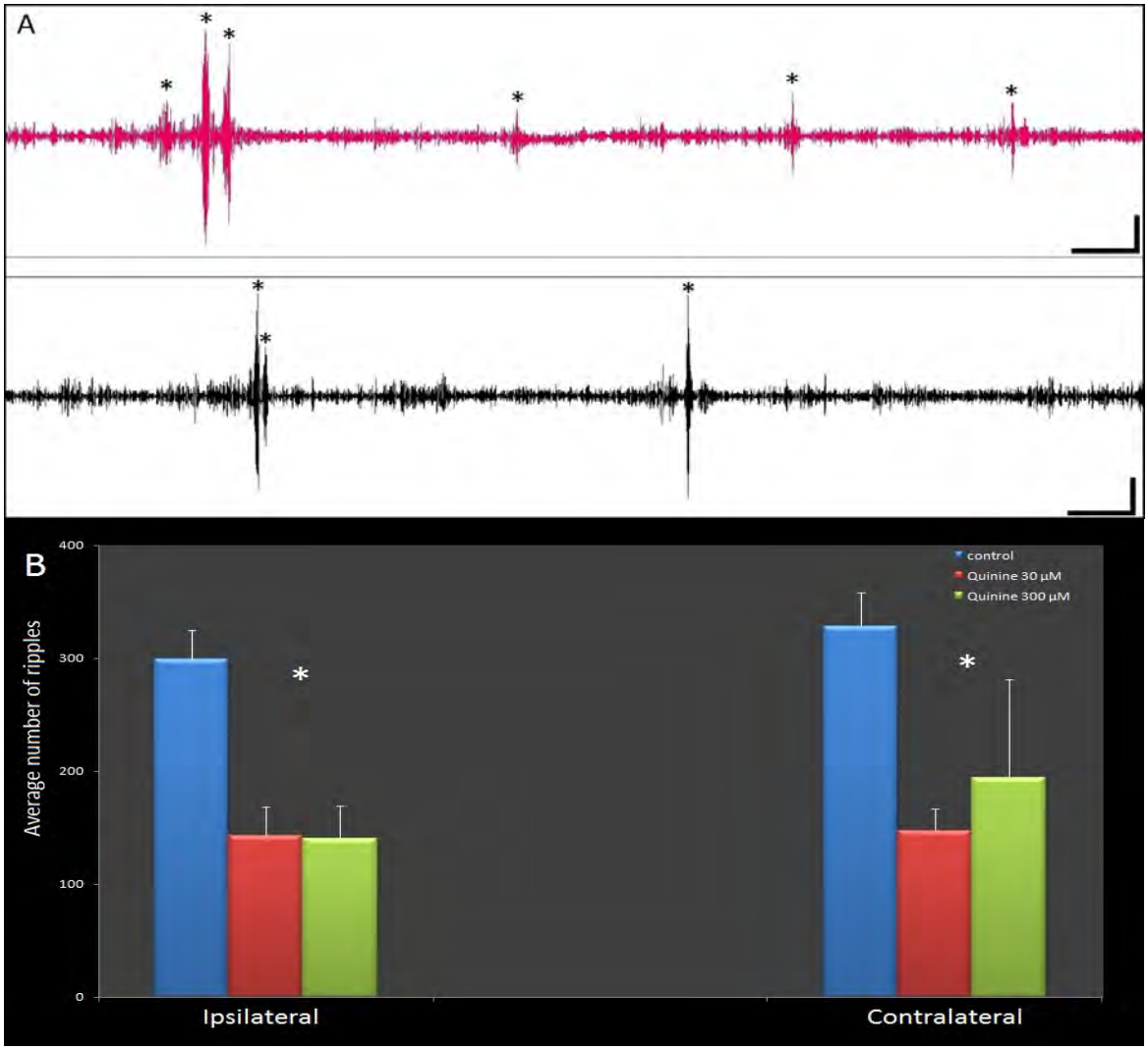

Fig.11: Ripple count for Quinine experiments***. A***: Local field potential recorded from the drug-injected hippocampus and filtered between 80 and 200 Hz in order to show ripple activity. The upper trace (red) shows activity recorded following control injection, while the lower trace (black) shows the reduction of ripple episodes following injection of Quinine 30 μM. A similar behaviour was found for the contralateral hippocampus, as well as for ipsi- and contralateral hippocampus for the higher Quinine concentration used in this study (300 μM). Asterisks mark the occurrence of ripple episodes. Calibration marks: horizontal: 0.5 s; vertical: 0.5 mV. ***B***: total ripple count in a 10 minutes time window averaged per number of animals. The number of ripples recorded under Quinine infusion decreased to about 48 and 47% of control values in the injected side, while the ripple count for the contralateral hippocampus decreased to about 45% and 59% of control values. Asterisks mark statistically relevant differences ($p<0.05$, n=7).

The decrease in the number of ripples observed for the ipsilateral side was preserved in the contralateral side, where I recorded 328.0 ± 30.3 ripples under control as opposed to 147.1 ± 20.0 and 194.4 ± 86.9 following Quinine 30 and 300 μM injection, respectively, a decrease to about 45 and 59% of the control for that side of the hippocampus. ***Fig.11A*** depicts two sample traces from animals treated with control (red trace) and Quinine 30 μM (black trace), while ***Fig.11B*** reports the number of ripple episodes recorded, averaged per number of animals, in control versus drug-injected conditions for the ipsi- and contralateral hippocampi. No statistically relevant difference was found between recordings performed in the same condition (i.e., ipsilateral control Vs. contralateral control; ipsilateral Quinine Vs. contralateral Quinine), but I observed a relevant decrease in the number of ripples observed for control Vs. Quinine in both the concentrations used and in both sides of the hippocampus (paired t-test, $p<0.05$, n=7).

I then performed a detailed analysis of the distribution of ripple length. I found that about 98% of the ripples recorded had a length comprised between 50 and 130 ms (data not shown). Therefore, for simplicity I focused analysis on this length interval. Upon normalization to the number of ripples recorded, I observed a Gaussian distribution of the length of the episodes in both control and drug injected conditions. In control condition, I observed that the distribution of ripple length peaked at 70 ± 5 ms for the ipsilateral and contralateral side. Upon drug injection, I found that the length distribution peaked between 75 ± 5 ms for both sides of the hippocampus and for both the Quinine concentrations used in this study. These findings are shown as normalized distribution curves in ***Fig.12***. In order to evaluate any statistically relevant difference between control and drug-injected conditions, I performed a series of Kolmogorov-Smirnov two-sample test using the tools described in the method section. Since no statistically relevant difference was found for any of the conditions analysed, I concluded that Quinine is not able to influence the length of ripple episodes.

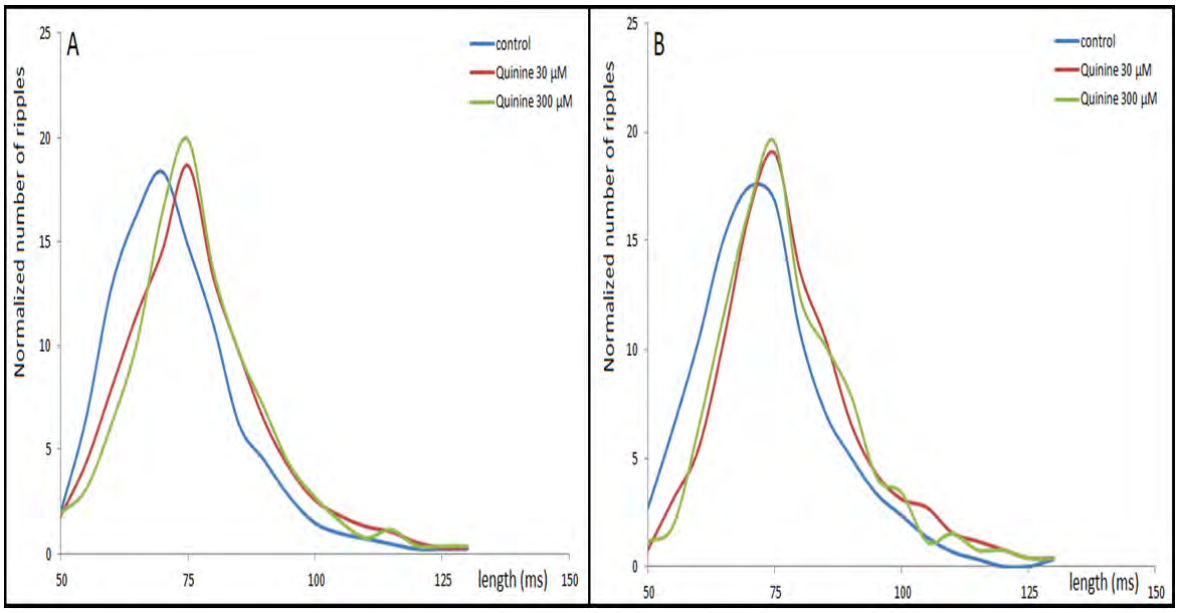

Fig.12: Normalized length distribution for Quinine experiments. ***A***: ipsilateral, injected side; upon injection of Quinine, there is a shift in the length of the ripple events to higher values for both the concentrations of Quinine used. ***B***: the same behaviour is observed in the contralateral side, but these effects were found not statistically relevant.

I then investigated the inter ripple interval (I.R.I.), which is to say the time elapsed between two consecutive ripple episodes. The I.R.I. showed a broad distribution, with episodes distant from a few milliseconds to well over 300 seconds. Such distribution is to be expected, because when animals were in a period of intense ripple activity, hundreds of such events could be recorded in a matter of a few seconds. On the other hand, when the animal was in theta activity ripples could still sporadically appear, but the I.R.I. could potentially be much longer since single ripples were much more sparse and distant from each other.

As shown in ***Fig.12A***, I.R.Is recorded after injection of control solution assumed a half-normal distribution, with ripple events that could be distant from < 1 s to well above 400 seconds from each other. Upon Quinine injection, I observed a displacement of the I.R.I. parameter towards lower values: ripples were fewer in numbers (as noted above) and they tended to more often appear closer to each other. This observation is represented in ***Fig13A'***, where I show that most if not all the ripples recorded under Quinine conditions had an I.R.I. below 300 seconds

(more evident in the normalized distribution in ***Fig.13B***). The same behaviour was observed for the contralateral hippocampus, although as shown in ***Fig.13B'*** the effect of the drug was not as pronounced as in the injected hippocampus (see also ***Fig.13C***). This effect also provoked the appearance of a higher number of ripple episodes clustered together (***Fig14A***).

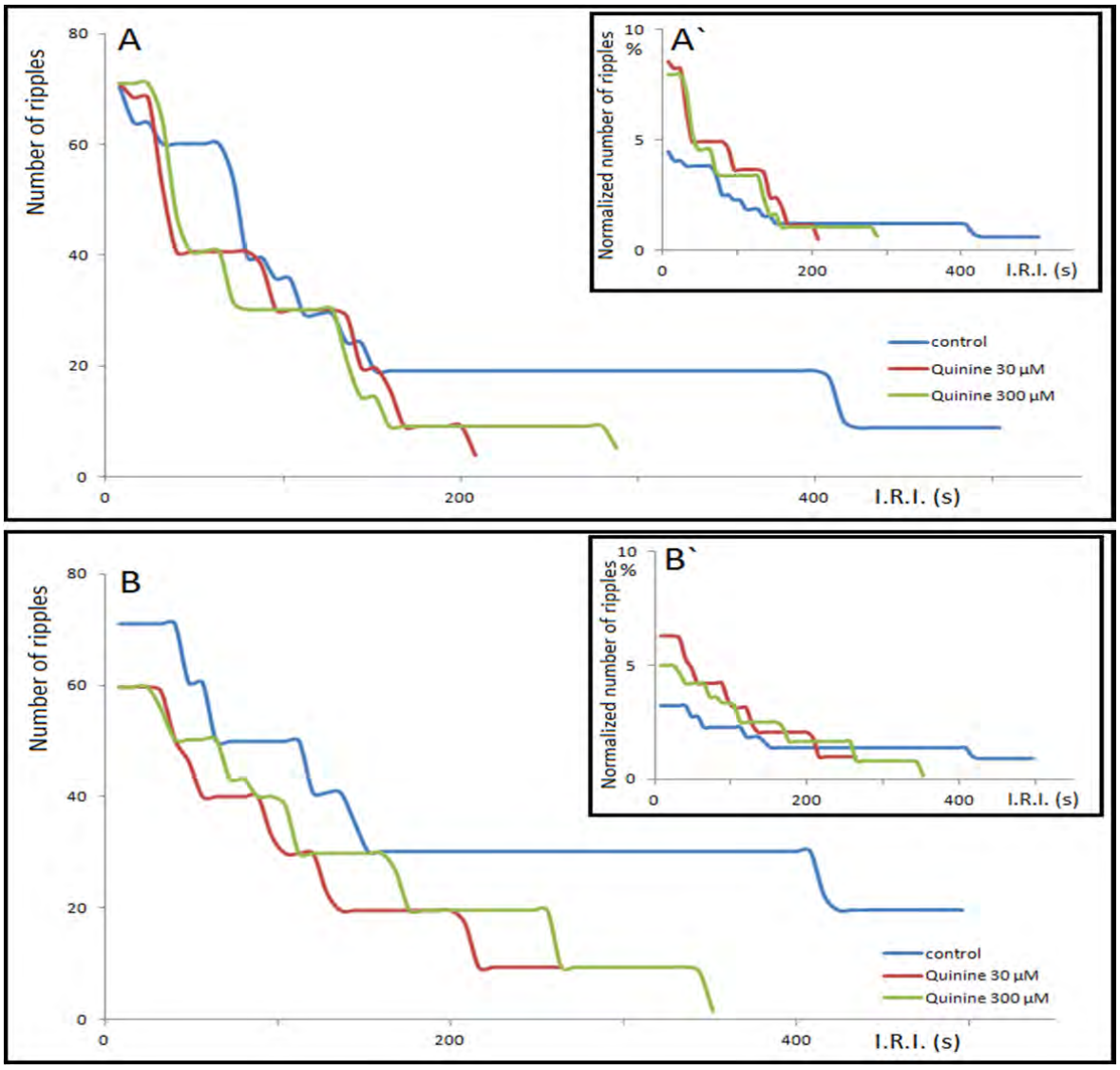

Fig13: Total number of ripples vs. I.R.I. ***A***: non-normalized distribution of ripple episodes recorded in different conditions vs. the I.R.I. As observed, upon Quinine injection ripple episodes with longer inter ripple intervals (>300 s) tend to disappear. ***A'***: normalized number of ripples vs. I.R.I.: the disappearance of longer inter ripple intervals leads to an increase in the number of ripples with I.R.Is below 150 s. The same behaviour was observed for the contralateral side (***Fig.13B*** and ***B'***).

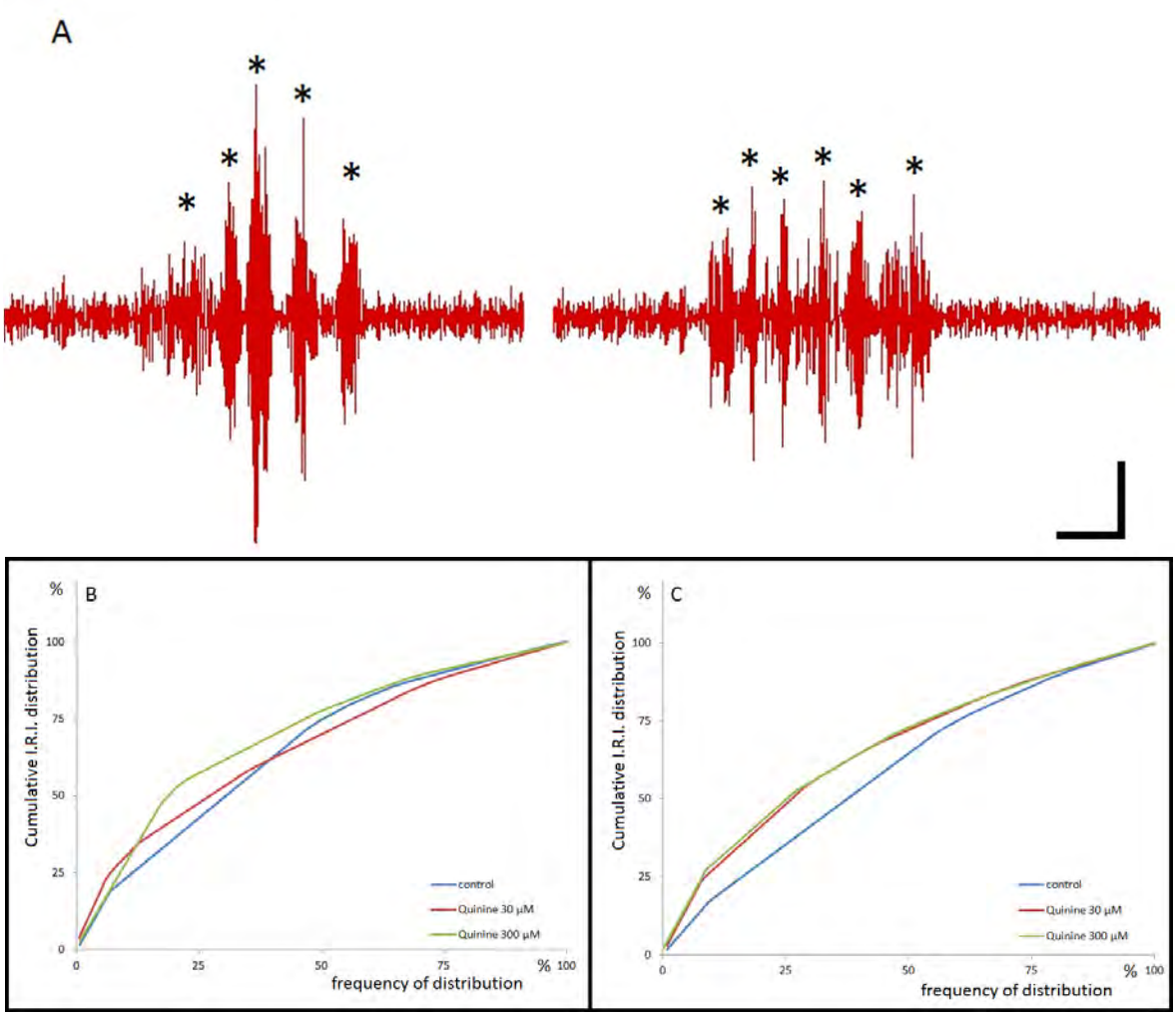

Fig.14: Ripple clusters and cumulative I.R.I. distribution. ***A***: Sample of ripple clusters. The figure shows clusters of ripples recorded from the injected hippocampus of different animals, in different conditions: Quinine 30 µM, left trace; Quinine 300 µM, right trace. A similar behaviour was observed for the contralateral hippocampus. Clusters of ripples could also be observed under control conditions, though not as frequently. Asterisks mark the occurrence of ripple episodes. Calibration marks: horizontal: 0.2 s; vertical: 0.5 mV. ***B***, ***C***: Cumulative ripple distribution for Quinine in the injected (left) and the contralateral hippocampus (right). Under drug injection, the ripple population undergoes a leftward shift towards lower I.R.Is, evident as an increased steepness of the cumulative curve vs. control. This shift was found to be statistically relevant and preserved for both concentrations of Quinine and for both the hemispheres of the hippocampus (see text).

Comparing the various population distributions through the two-sample KS, I found that in the injected hippocampus there is a significant difference in the cumulative I.R.I. distribution between control and Quinine conditions (P=0.001 and 0.008 respectively for Quinine 30 and 300 µM population distribution vs. control distribution; ***Fig.14B***). This significance is preserved in the contralateral side (P=0.001 for both Quinine concentrations used vs. control population;

Fig.14C). From these analyses, I concluded that Quinine, in both the concentrations used in this study and in both hemispheres of the hippocampus, is able to decrease the interval between two consecutive ripple episodes. This decrease takes the shape of an increase in the steepness of the cumulative curves for Quinine conditions as opposed to the curve for the control distribution.

I then moved to investigate whether Quinine was able to produce changes in the frequency and in the amplitude of the ripple events, but I did not find any statistically relevant difference between the control condition and recordings obtained following injection of the drug in both the concentrations used (data not shown).

Substance P

In a different set of experiments, I investigated whether the peptide Substance P was able to provoke changes in the various parameters taken under consideration. First, I considered the total number of ripple events recorded under control conditions and upon drug injection. In a 10 minutes time window, I recorded an average of 282.7 ± 23.8 and 254.6 ± 41.3 ripple events for the control injected and the contralateral side of the hippocampus, respectively. Upon injection of Substance P, the average number of ripple episodes recorded per animal decreased to 274.6 ± 28.0 in the injected side (90% of the control value). On the other hand, I observed that the ripple episodes in the contralateral side experienced an increase to 433.8 ± 66.5 (158% of the control value). As ***Fig.15A*** illustrates, part of this increase was due to the appearance in the contralateral side of ripple episodes that were not present (hence non-detectable) in the ipsilateral side. No relevant difference was found between control and SP injection for the ipsilateral hippocampus. On the other hand, I observed a statistically relevant increase in the number of ripples recorded in the contralateral side following SP injection (SP injected in the ipsilateral side: $p<0.05$, n=seven experiments). These observations are summarized in ***Fig.15B*** in the following page.

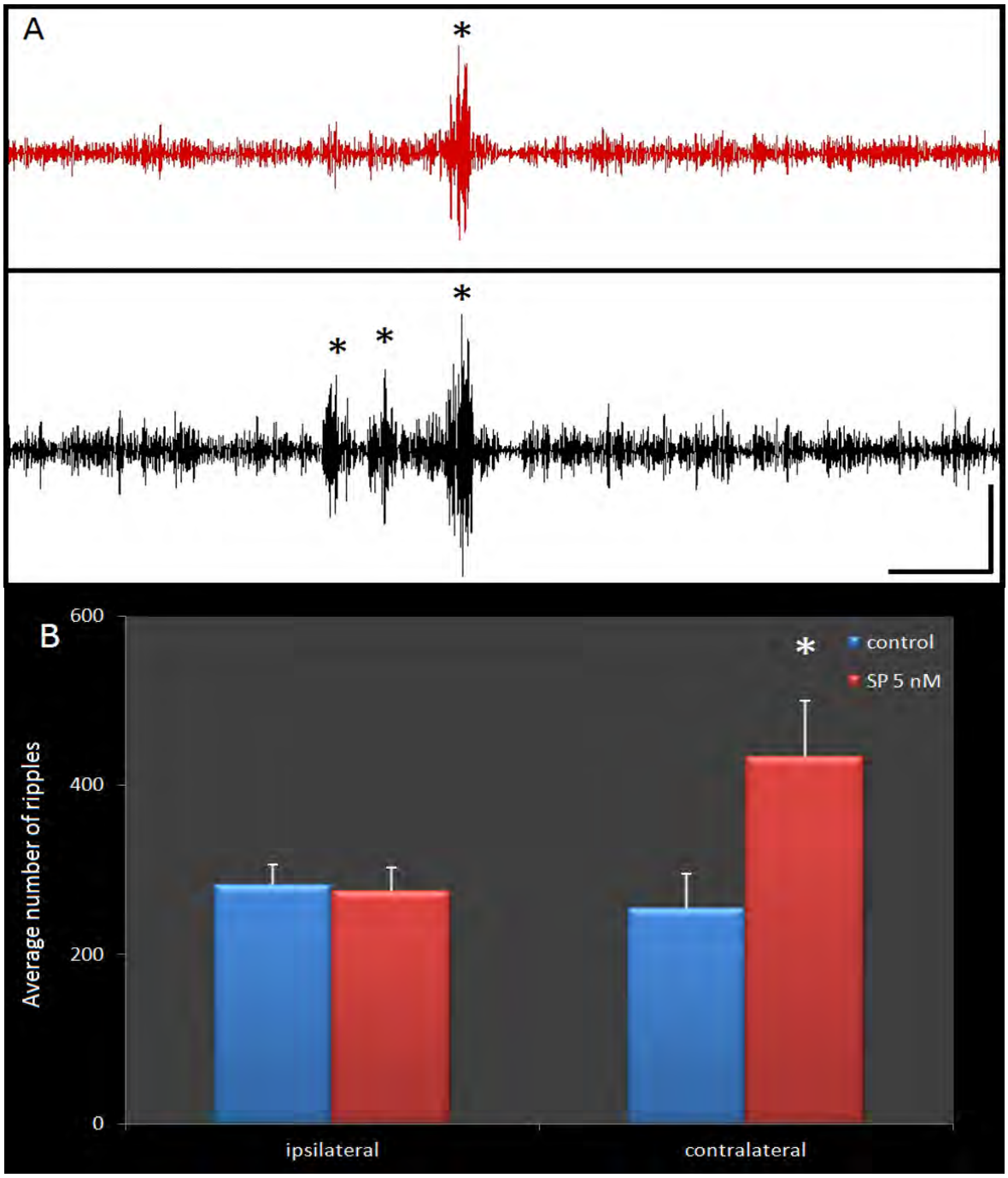

Fig.15: average number of ripples in control vs. SP injection. ***A***: Local field potential recorded from the drug-injected hippocampus and filtered between 80 and 200 Hz in order to show ripple activity. The upper trace (red) shows ripple activity recorded following Substance P injection in the ipsilateral hippocampus, while the lower trace (black) shows the concomitantly recorded ripple activity in the contralateral side of the same animal. Asterisks mark the appearance of ripple episodes. Calibration marks: horizontal: 0.5 s; vertical: 0.5 mV. ***B***: Average ripple count in a 10 minutes time window recorded in control condition (blue bars) and upon injection of SP (red bars). After SP injection, I observed a significant increase in the number of ripples recorded in the contralateral hippocampus, but not in the injected side. Asterisk marks the statistically relevant difference ($p<0.05$, n=7).

Next, I analysed the length distribution of the recorded ripples. As for the Quinine experiments, I observed a Gaussian distribution of the length of the episodes in both control and drug injected conditions. In a similar manner to the Quinine experiments, I observed that the distribution of ripple length both for the injected and contralateral hippocampus peaked at 75 ± 5 ms under control conditions. I observed a similar distribution following SP injection (***Fig.16A*** and ***B***). I also observed some slight differences in both hippocampi when comparing the two Gaussian distributions for control and drug conditions (especially in the case of the contralateral side, ***Fig.16B***). In order to evaluate whether these differences had any statistical relevance, I run a series of KS tests on the ripple populations recorded in the various conditions. These analyses revealed no statistically significant divergence between any of the conditions analysed (two-sample KS test; P values= 0.673 for control Vs. SP injection, both ipsi- and contralaterally). I therefore concluded that Substance P is not able to relevantly affect the length of ripple episodes.

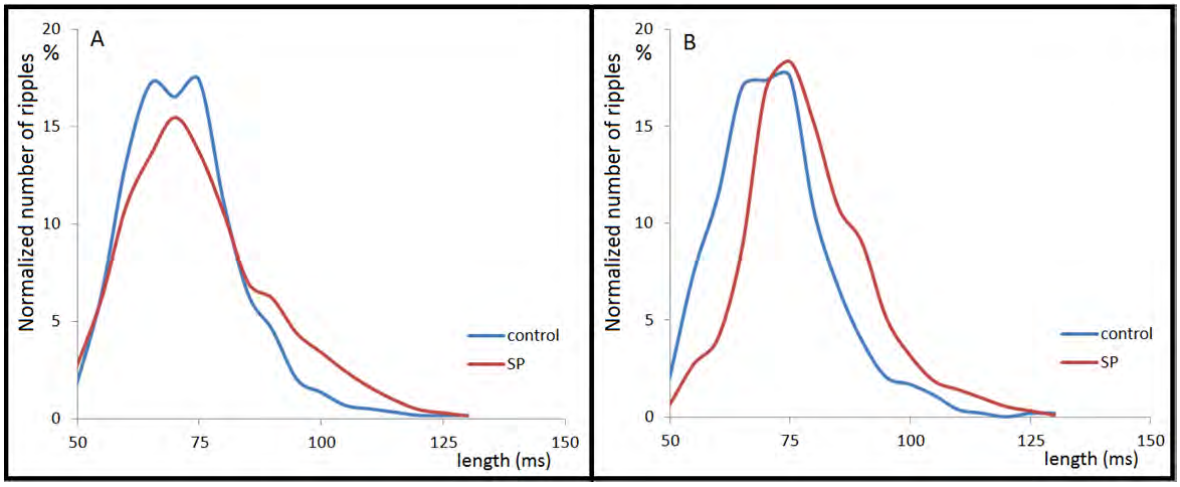

Fig.16: normalized length distribution for ripples recorded under SP injection. ***A***: injected hippocampus. Upon injection of SP, I observed a decrease in the number of ripples for the central part of the Gaussian distribution and an increase in the percentage of ripples with higher lengths, in line with a general shift of the ripple population towards higher durations. ***B***: contralateral hippocampus. Also in this case I observed a general shift of the entire ripple population towards higher lengths. Upon further analyses, these differences were revealed non-significant.

As shown for the Quinine experiments, I then investigated the I.R.I. Again, this parameter showed a broad distribution given by the appearance of periods of intense ripple activity interrupted by periods of theta activity; this tended to elongate the average I.R.I.

I found that the average I.R.I. recorded under control conditions was 39.3 ± 25.9s for the injected hippocampus and 35.6 ± 18.4s for the contralateral. Following SP injection, these values increased to 40.9 ± 26.0s for the injected side and 61.5 ± 25.7s for the contralateral side (***Fig.17***).

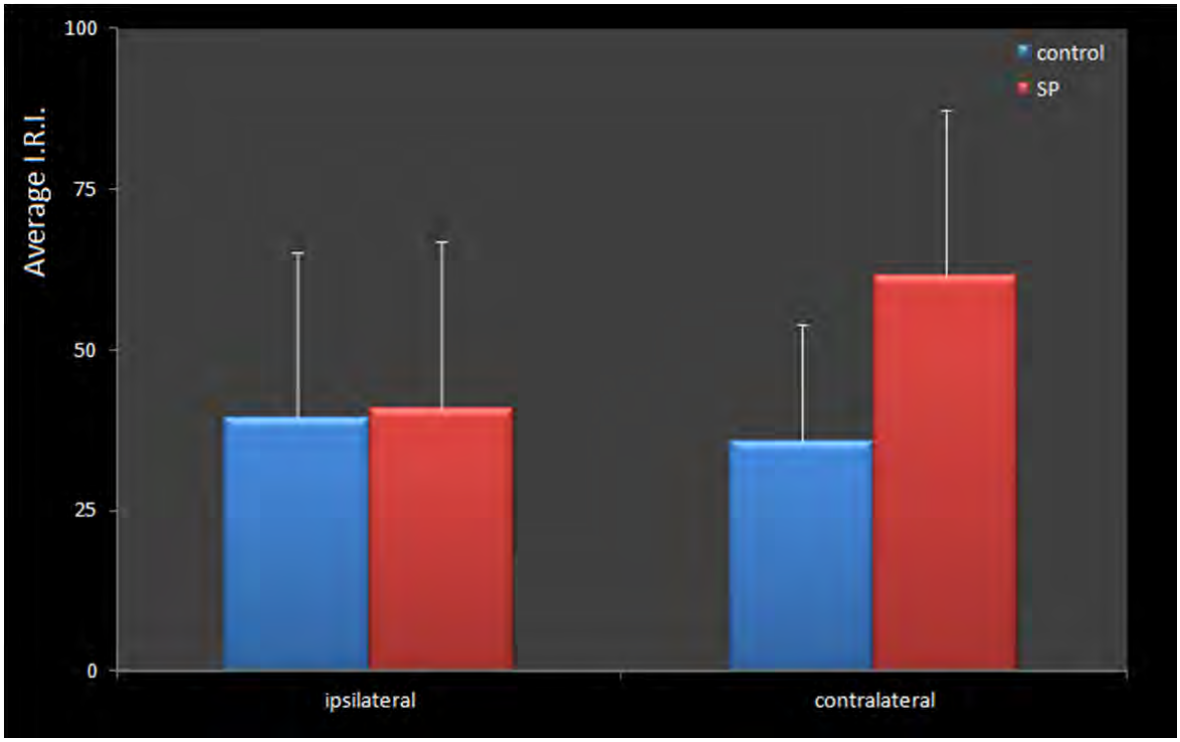

Fig.17: average I.R.I. following SP injection. I found that there is no variation in the average time interval between two consecutive ripple episodes for the injected hippocampus (ipsilateral, left), while there is a non-significant increase for the contralateral side (contralateral, right).

To investigate whether SP was able to promote a possibly statistically relevant modification in the I.R.I., I compared the I.R.I. cumulative distribution of the various populations (***Fig.18***), analyzing these populations through a KS test. With this method I observed that there was no relevant difference between control and SP neither for the injected side (P=1.00), nor for the

contralateral hippocampus (P=0.84). These observations led us to conclude that the peptide Substance P has no obvious effects on the inter-ripple-interval of ripple episodes.

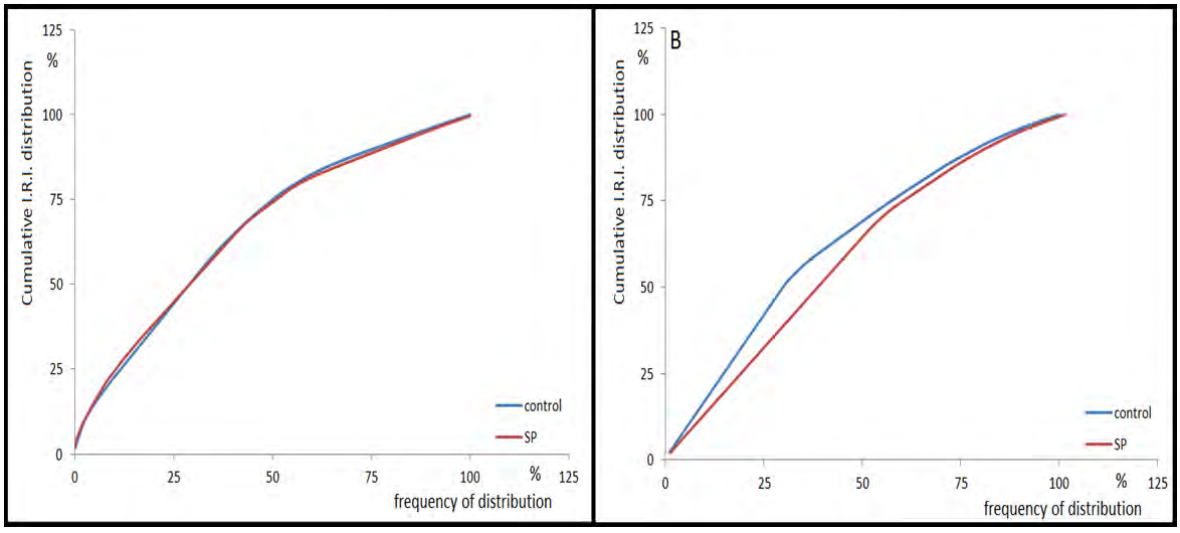

Fig.18: Normalized cumulative I.R.I. distribution for SP experiments. ***A***: for the injected hippocampus, the control and SP populations overlap and there is no clear difference in distribution. ***B***: In the contralateral side, I observed a rightward shift in the I.R.I. population distribution, consistent with an increase of the I.R.I. upon drug injection. Nonetheless, the effect of the drug was found to be non-significant.

I then investigated the influence of SP on the amplitude of the ripples. The amplitude correlates to how strong the ripple appears: the stronger the amplitude of the ripple event, the easier it is to detect the episode in the unfiltered and filtered local field potential. Ripple amplitude could nonetheless be biased by the distance between pyramidal layer and recording electrode. In order to standardize amplitude analysis, I employed in my analysis recordings obtained from channels which recorded activity from the pyramidal cell layer. The method is reported in the appropriate section in the “Materials & Method” section. Additionally, to further validate this approach, I performed an inter-hemispheric comparison of ripple amplitude in control conditions. The rationale behind this was that if the channels selected for the comparison were not located in the pyramidal cell layer, I would have observed evident differences in the ripple populations' distributions under control conditions between the two hemispheres.

Fortunately, this was not the case (***Fig.19***), since the KS test for the two control conditions returned non-significant (P=0.563). It was then concluded that the selected channels were genuinely placed in the same hippocampal layer, which as explained in the method section was assumed to be the pyramidal cell layer.

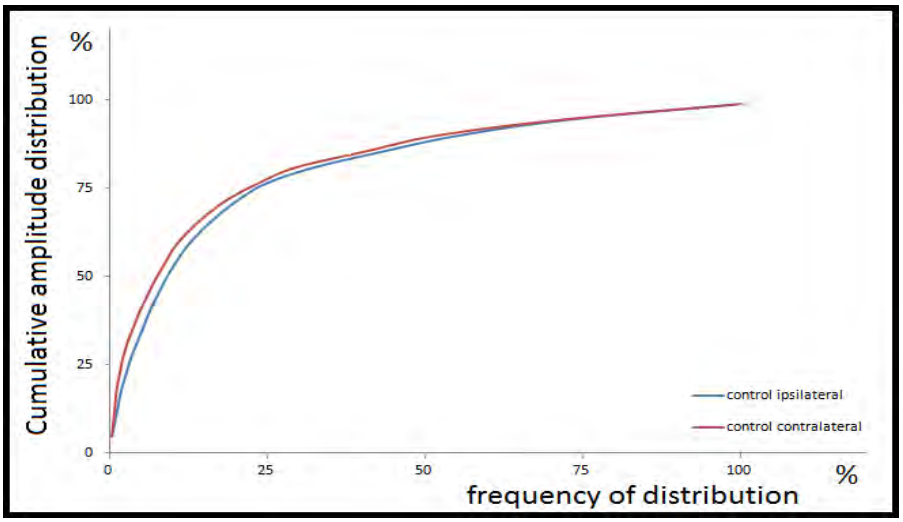

Fig.19: Cumulative amplitude distribution for ripples recorded under control conditions for ipsilateral and contralateral hippocampus. The two curves almost totally overlap, indicating that the ripple populations were both recorded from the same layer, which was assumed to be the pyramidal cell layer. This indicates that the method of channels selection is not influenced by electrode positioning (see text for details).

Analysing the recorded traces with this method, I was able to record ripple events with amplitude between 0.8 and 5 mV, leading to a Gaussian distribution of the ripple population (***Fig.20A*** and ***B***). In control conditions, the amplitude peaked at 1.0 ± 0.2 mV for both the injected and contralateral side and the same distribution was found upon injection of Substance P. Even though the curves peaked at the same value, I observed relative differences in the distribution of ripple amplitude between control and SP injection. To further characterize these differences, I performed once again a series of KS tests on the different populations. From these tests, it appears that there is no statistically significant difference in ripple amplitude between control and SP injection for the ipsilateral side (P=0.979, ***Fig.20C***). I also observed a non-relevant divergence in the amplitude distribution between control and SP injection for the

contralateral side (P=0.821, ***Fig.20D***). It was then concluded that SP is not able to modify the amplitude of ripple events.

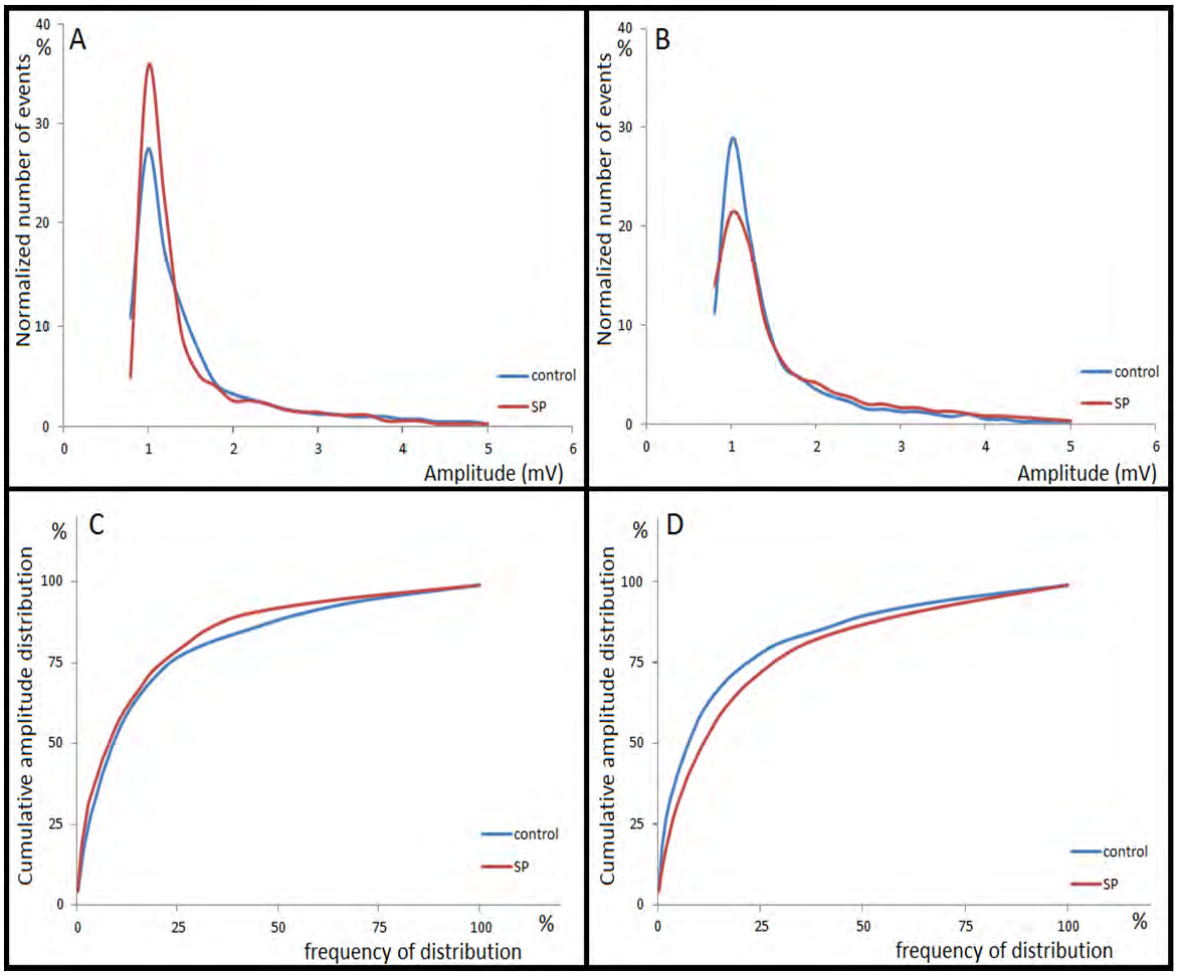

Fig.20: Normalized amplitude distribution for SP experiments. ***A***: upon SP injection, I observe a decrease of ripples with amplitude of 0.8 mV, while there is a higher occurrence of ripples with amplitude of 1 mV. ***B***: the pattern is reversed in the contralateral side. This different behaviour led to compare the cumulative populations' distribution, as shown in panels ***C*** and ***D*** for the ipsilateral and contralateral side, respectively. I observed no relevant differences in the amplitude population distribution for any of the aforementioned conditions.

I then moved to analyse the frequency distribution of the ripples episodes. Ripples in the hippocampus usually have a frequency between 80 and 200 Hz. Higher frequencies could also appear: as a matter of fact, some researchers have reported the appearance of ripples in frequencies up to 500 Hz, but these works focused on kainic acid-induced epileptiform activity in rodents [100, 101] or patients with mesial temporal lobe epilepsy [100, 102, 103]. It is

therefore entirely plausible that these fast ripples are a by-product of the induced or innate pathological condition and are not to be found in a healthy organism. Since this assumption is currently debated, I decided to analyse ripples frequencies in accordance to what it is commonly accepted to be the physiological range of such events: 80-200 Hz.

I differentiated the frequencies of the various ripple events and categorized them in seven groups, 20 Hz away from each other. For simplicity, I will refer to the various groups with the middle frequency in the 20 Hz window, which is to say that the range of frequencies between 130 and 150 Hz will simply be referred to as the 140 Hz peak or group.

After normalization, I observed a skewed Gaussian distribution of the frequencies in the control conditions, in both the injected and the contralateral hippocampus (***Fig.21***, blue bars). This distribution peaked at 100 Hz (90 to 110 Hz frequencies), with smaller values for frequencies both above and below 100 Hz. This peak accounted for 26.5 ± 6.1% and 30.4 ± 6.2% of the ripple frequencies population for the control recording in the ipsilateral and contralateral side, respectively.

Analysing the frequency distribution upon injection of Substance P, I found a very similar pattern, with once again a strong peak appearing for frequencies around 100 Hz (23.5 ± 4.5% and 30.8 ± 5.8% for ipsilateral and contralateral side, respectively; ***Fig.21***, red bars). I did not observe any relevant difference between control and SP recordings neither for the injected side nor for the contralateral side of the hippocampus. I therefore concluded that SP injection does not produce changes in the ripples frequency.

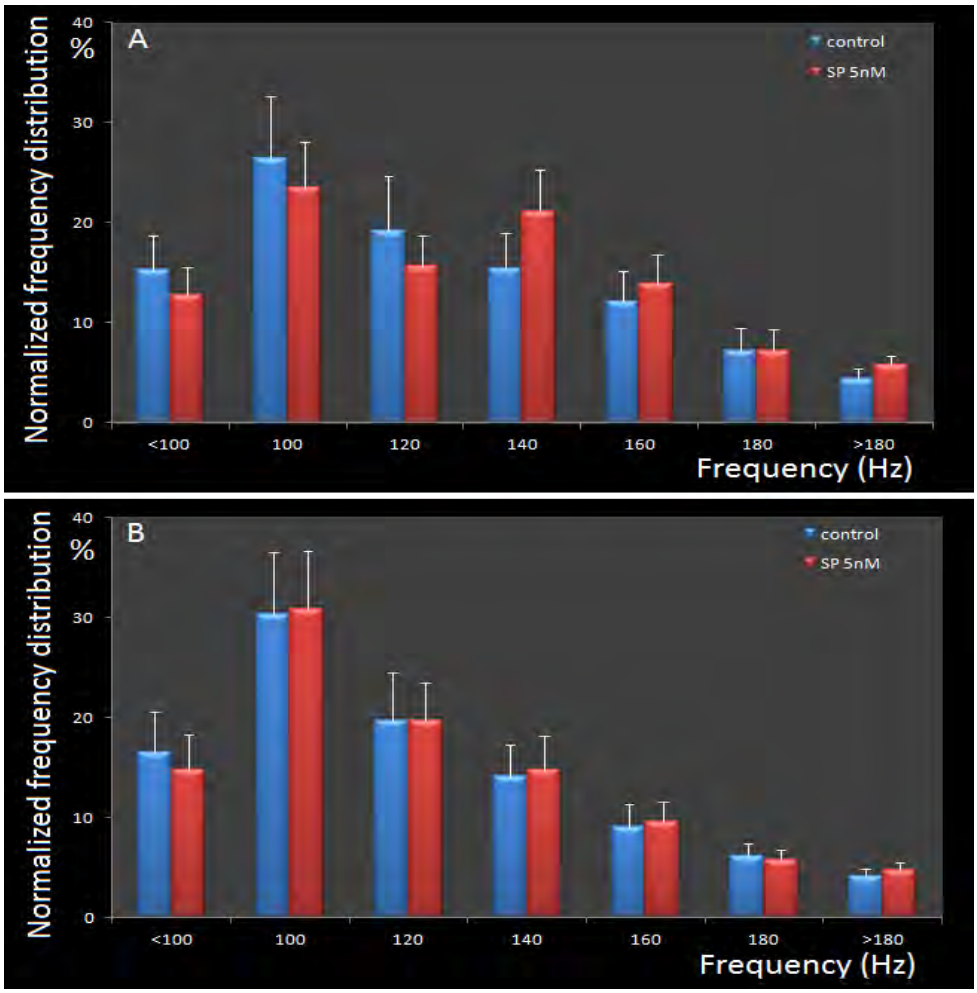

Fig.21: normalised frequency distribution for SP experiments. ***A***: ipsilateral side; I observed a peak for the 100 Hz group (90 to 110 Hz ripples) in both the control (blue) and the SP recordings (red). ***B***: contralateral side; I observed a very similar distribution of ripples frequency, once again with a strong peak for the 100 Hz group. No statistically evident difference was found in any of the groups considered.

DISCUSSION

General considerations

This work focused primarily on the analysis of ripple activity in the rat's hippocampus, *in vivo*; in particular, the aim of the work was to investigate whether ripple activity in one hippocampus is controlled or influenced by long-projecting interneurons, whose somata reside in the opposite hippocampus.

Based on their axonal arborisation, inhibitory cells in the hippocampus can be divided into local circuit cells (< 1 mm) and long-projection neurons (> 1 mm) [44, 50, 104]. The long-projection group includes bistratified cells, trilaminar and back-projection interneurons. Since long-range interneurons branch in a much larger volume than local circuit cells, it has been suggested that this sub-population of inhibitory cells might be able to exert a more global effect on their targets than local circuit interneurons [44]. This is because while a typical local circuit cell innervates ~1500 pyramidal cells [44], it has been estimated that long range inhibitory cells have 15,000-20,000 synaptic contacts [44, 50]. These numbers indicate that even a single long-projection neuron can have a significant impact on the regulation and/or synchronization of a large number of excitatory neurons, especially if it predominantly innervates local circuit inhibitory cells. As a matter of fact, it was recently reported that hippocampo-septal long-projection neurons preferentially innervate local circuit interneurons in the hippocampus [51]. This population of neurons contain Neuropeptide Y (NPY), Somatostatin (SOM) and Calbindin (CB) [49, 51]. The CB/SOM-containing cells do not have extensive axonal arborisation in the hippocampus and do not project to the contralateral hippocampus, only to the medial septum [49]. The other population expresses NPY. Unpublished data from Dr Sik's laboratory revealed that a subpopulation of NPY-immunoreactive inhibitory cells, located in the CA1-CA3 regions

as well as in the dentate gyrus, present large local axonal arborisation in the hippocampus, project to the septal regions and importantly have a massive axonal projection to the contralateral hippocampus. Target analysis also revealed that local circuit PV-IR neurons, likely basket cells, are among the targeted cells. It is therefore plausible that NPY-expressing cells play a key role in the hippocampal oscillations' synchronization.

To investigate this role, I performed recordings of ripple events before and after injection of specific drugs, monitoring hippocampal ripple activity in both the injected and the contralateral hippocampus. The rationale behind these experiments was that, if indeed long-range projecting neurons synchronize or help in synchronizing ripple activity in one side of the brain, these cells might be able to exert the same action in the contralateral side. If so, acting positively or negatively on the inhibitory network in one hippocampus might lead to changes in the ripple activity in the contralateral hippocampus.

In order to influence the inhibitory network's activity, I injected Quinine and SP in one hippocampus. Quinine is known to disrupt the gap-junction coupling between inhibitory cells [91, 92] while Substance P has been reported to enhance the performance of the inhibitory network, increasing the frequency of spontaneous GABAergic events and reducing that of spontaneous glutamatergic events [85, 86, 89, 93, 105-107].

In my view, local disruption of the gap-junction coupling would affect ripple activity in the injected hippocampus, but not in the contralateral hippocampus. This is because gap-junctions have been observed only between local circuit interneurons [108], but to date evidence is still missing about gap-junctions in long-projection neurons. On the other hand, injection of Substance P would likely strengthen the inhibitory network in both the injected and the contralateral hippocampus through long-projecting interneurons. In the contralateral side, I therefore would have expected to observe changes in the analysed ripple parameters following SP injection, but not following Quinine injection.

Quinine

In accordance to my original hypothesis, following Quinine injection I observed a clear decrease in the recorded ripple events in the ipsilateral hippocampus (***Fig.11***). This drug acts blocking Cx36 gap-junctions between inhibitory neurons [91]; since Cx36 plays a major role in the inter-communication between interneurons, the disruption of this cross-talk system would lead to an overall excitation of the inhibitory network. Maier and collaborators published a similar observation showing that in Cx36 knockout mice, ripple events were fewer in numbers [56]. My results are in line to a certain extent with these findings, since I observed a reduction of ripple episodes following Quinine injection in both ipsilateral and contralateral hippocampus. To explain the mechanism through which Quinine would act one must keep in mind that interneurons in the hippocampus are by definition, inhibitory in nature. Coupled with the notion that Cx36 gap-junctions have been demonstrated to exist between inhibitory cells [70], this leads to the existence of a population of interneurons whose role is to modulate the activity of the inhibitory neurons they contact. Quinine, along with other connexin blockers, is able to perturb this modulation. Lifting this natural brake leads to an overall excitation of the inhibitory network. The increased excitation would in turn lead to a less efficient recruitment of excitatory neurons, which would translate in fewer, weaker and/or more disperse ripple episodes. My original assumption was that Quinine would only act ipsilaterally on PV-IR basket cells, which express Cx36 and are connected among each other by chemical synapses [65-67, 71]. Changes in ripple parameters recorded in the ipsilateral side would not be transferred to the contralateral side, because prior to this work no evidence was produced on the existence of gap-junctions between local circuit and long-projection interneurons.

Along with the expected decrease in the number of ripples recorded in the ipsilateral side, I observed that the decrease of ripple activity is preserved also in the contralateral side (***Fig.11***). The data seem to point out that a local injection of Quinine in the CA1 area is able to disrupt

generation of ripples from the CA3 area. This could be due to a feedback mechanism from CA1 to CA3 pyramidal cells, or alternatively the disruption could be modulated by long projection neurons, which reside in the CA1 area and have extensive axonal terminals in the CA3 area as well. This hypothesis would also explain why I observed a reduction of ripple episodes in the contralateral side, since long-range interneurons project massively to the contralateral CA3 area. If this were the case, neurons responsible for influencing ripple activity in both hippocampi would need to express gap-junctions. Even if to date no clear evidence has been produced to show that long projection neurons express gap-junctions, there is evidence that expression of Cx36 is not exclusive to PV-IR basket cells; other kind of interneurons, both in the cortex [109-111] and in the hippocampus [112, 113] have been shown to express these proteins.

In their *in vitro* study, Maier *et al*. did not focus on the ripple parameters investigated in this study, but they report that frequency of ripples was substantially decreased in Cx36 KO mice [56]. I was not able to repeat this observation *in vivo*, probably because I focused my analysis on the physiological ripple frequency (80-200 Hz), in opposition to the frequency range used in their study (90-500 Hz). In any case, following either Quinine injection (this study) or deletion of Cx36 [56], the increased excitation of the inhibitory network appears to be perceived by the hippocampus as an insult to the entire network, similar to what happens under pathological conditions such as Epilepsy. The disappearance of the longer I.R.Is, which as addressed below might be linked to little theta activity in Quinine treated animals, also points in this direction. I speculate that widening the analysis window above the canonical 80-200 Hz frequency might lead to observation of unnatural ripple frequencies, a by-product of un-physiological conditions. If this were true, I would expect to observe a marked reduction in ripples having a frequency above 200 Hz, because it is considerably more challenging for the network to synchronize a sufficient number of neurons to fire at above 200 Hz frequencies, especially in view of the hyper-excitation of the inhibitory network following gap-junction blockage.

Analysis of the various ripple parameters showed no clear differences between control and Quinine injection for the length of the ripple episodes (***Fig.12***). Ripple length is influenced by how many pyramidal cells are recruited for the episode. During ripples, two antagonistic polarizations compete with each other to drive firing of CA1 pyramidal cells: dendritic excitation from the CA3 neurons and somatic/perisomatic inhibition from local projecting interneurons. Dendritic depolarization is a direct consequence of the excitatory drive on CA1 neurons from CA3 pyramidal cells, while axon terminals of basket and chandelier cells can induce somatic and axonic inhibition of CA1 pyramidal cells concomitantly with dendritic excitation. While the generation of a ripple episode is considered responsibility of CA3 pyramidal cells, rhythmic and coherent firing of interneurons is responsible for the timing of action potentials of CA1 pyramidal cells during ripples. This is also demonstrated by the fact that interneurons generally fire one to two milliseconds after pyramidal cells during a ripple episode [7]. Keeping these observations in mind, the failure in observing any differences in ripple length between control and drug injection seem to point out that interneurons do not play a role in modulating the length of the episode, but are only responsible in synchronizing the coherent firing of the pyramidal cells population while the ripple episode is still ongoing.

On the other hand, if ripple episodes were equally distributed throughout the recorded activity of the animal, the observed decrease in the numbers of ripple episodes would lead to an increase in the time elapsed between two consecutive ripples. However, what I observed is that after Quinine injection there was an overall decrease of the I.R.I. (***Fig.13***). This decrease upon further analysis was found to be in small part due to a decrease in the shorter I.R.Is (i.e., disappearance of ripples recorded during non-theta activity). This is important because a decrease in the total number of ripples following drug injection would have likely affected ripples recorded both during non-theta and theta activity. Instead, I observed an almost total disappearance of ripples during theta activity (which present longer I.R.Is) as well as an

increased number of ripple clusters (***Fig.14A***). The increase in ripple clusters could probably be explained considering that Quinine, along with its well-documented blockage of Cx36, may have other unspecific effects. As an example, it was demonstrated that the drug could block the activity of TWIK-1 and TREK-1, two potassium channels expressed by astrocytes in the hippocampus [114]. Since astrocytes are involved in potassium siphoning [115] and spatial buffering [116], it is plausible that a blockage by Quinine of the inwardly rectifying K^+ channels would affect the ability of astrocytes to distribute potassium after intense neural activity (such as ripples). This would in turn increase the extracellular potassium concentration, with the result of a blockage by depolarization of pyramidal neurons: pyramidal cells would fire intensely for a brief period of time, and then block for a longer period because the extracellular potassium concentration is too high to sustain additional firing. An additional explanation could be that Quinine acts on many different types of inhibitory neurons, some of which might be involved in mechanisms that allow the hippocampus to transit from a non-theta to a theta activity. I did not quantify theta vs. non-theta activity in my experiments, but if this were true, I would predict a higher ratio (theta vs. non-theta) for control recordings vs. drug treated animals.

In light of the information above, I suggest that long projection neurons form gap-junctions with local circuit inhibitory neurons. This fast method of communication would be used to monitor the overall activity of the hippocampus and to condition the generation of ripples by acting on inhibitory local circuit cells residing in the CA3 area. The potential influence of long-projection neurons on ripple generation would extend to the CA3 area of the contralateral side too, with similar results. It is possible likely that these putative gap-junctions are constituted by Cx36 monomers, as this would explain why Quinine affects them [91]. It is also that other proteins constitute these putative gap-junctions, on which Quinine-based drugs might also have an effect. In fact, although several antimalarials used as gap-junction blockers have been shown to interact preferentially with Cx36, these drugs are also known to associate with and block other

Connexins to a certain extent [92, 117]. Nevertheless, long-range neurons seem to be involved in ripple generation probably through a feedback mechanism involving CA3 interneurons and pyramidal cells.

Substance P

Following Substance P injection, I first analysed the total number of ripples recorded in the injected and the contralateral hippocampus. It is well established that SP promotes a reinforcement of memory formation and spatial navigation [93, 105, 106]; since ripples are thought to be involved in processes of memory consolidation both in rodents [118, 119] and in humans [120], I would have expected to observe modifications in ripple activity following administration of SP. The original assumption was that injection of SP in the ipsilateral hippocampus would lead to changes in the ripple parameters in both sides. More specifically, I would have expected to observe an increase in the number of ripples generated in both hippocampi. Contrarily to my predictions, I observed no change in the number of ripple episodes for the injected side and an increase in the contralateral side (***Fig.15***). It is plausible that the original assumption was based on an over-simplified approach, which I later found to be partially incorrect. I address and discuss a likely explanation for the discrepancy between the original predictions and the observations in the following paragraphs.

Expression of the Substance P receptor Neuro-Kinin 1 (NK1) was reported to be highest in the subiculum and the dentate gyrus, with lower expression levels in other hippocampal areas [79, 121]. In the CA1 field, Substance P receptors are expressed by several subpopulations of inhibitory cells. Acsádi *et al.* demonstrated that about 60% of NPY-IR, 20% of CCK-IR, 30% of CB-IR and 18% of SOM-IR interneurons express NK1 [122]. This means that the NK1 receptor is expressed by interneurons possessing a variety of immunochemical contents, axonal targets and electrophysiological behaviors [5]. Moreover, in the same study it was shown that

Parvalbumin immunoreactive (PV-IR) basket cells, which represent the largest population of inhibitory cells throughout the hippocampus [5], do not express Substance P receptors to any extent [122].

Among the neurons that express NK1 receptors, of particular importance for this dissertation are the NPY-IR. As already mentioned, NPY is expressed not only by the long-range projecting interneurons, but also by some bistratified neurons, which greatly increase their firing frequency during ripple episodes [123]. Keeping in mind the various populations that express NK1 in the CA1 area, I can approach to analyse what SP injection in the hippocampus would provoke.

SP increases the frequency of spontaneous GABAergic events, also reducing the frequency of spontaneous glutamate release [86]. Following injection, the peptide would increase the spontaneous release of GABA from all the neuronal populations that express the NK1 receptor. Among these, the NPY-IR long range projecting interneurons would respond to SP injection by strengthening their inhibitory drive on the interneurons they contact: Parvalbumin- and Colechistokynin-IR interneurons, among others.

My original assumption was that the increased inhibition on local circuit cells would lead in turn to a disinhibition (i.e., exacerbated excitation) of pyramidal cells. This is because the now inhibited local circuit cells would decrease their inhibitory drive on pyramidal cells, with the resultant effect of exciting the entire principal cells' population. The consequential network excitation would next lead to an increase in the number of ripples recorded. In light of my results, I believe that this disinhibition mechanism might still be valid for the contralateral, but not for the injected hippocampus. This is because in the contralateral hippocampus, which was not in direct contact with the drug, only terminals from NPY-IR long projecting neurons would be affected by SP. In the injected hippocampus on the other hand, Substance P would not only affect long projecting neurons, but also other populations of neurons as explained in details below.

In the ipsilateral side, although the disinhibitory effect addressed above might still be in place, the disinhibition mechanism would compete against the *direct* activation of NK1 receptors on other NK1-expressing interneurons. In particular, activation of the NK1 receptor on CCK-IR basket cells and bistratified neurons would lead to an overall excitation of these two populations of interneurons, leading in turn to a net increase of inhibition on principal cells. It is not known if these two opposing effects coexist or if one brings down the other. Nonetheless, keeping in mind that long range projecting neurons are thought to be few in numbers [44, 50] and that dendritic inhibition is generally considered to be weaker than somatic inhibition, it seems likely that the somatic and dendritic inhibition promoted by CCK positive basket and bistratified cells respectively would compensate and finally overthrow the disinhibition promoted by NPY-IR long projecting interneurons. This model seem to find support from my data, seeing as I found no difference in the number of ripples recorded between control and SP treated animals for the injected hippocampus. This observation points out that compensatory mechanisms are in place so that exacerbated activity from one group of neurons (in this case, NPY-IR long projecting cells) would be contrasted efficiently by other groups of cells (likely, Colechistokynin basket and bistratified neurons). The compensatory mechanisms would activate if a trigger (i.e., NK1 receptor activation), common to all cellular groups involved, promotes over-activation of the network.

In the contralateral hippocampus, the observations are easier to explain because neither bistratified nor CCK-IR local circuit neurons are *directly* affected by SP injection. As addressed above, the only neurons affected are long-projecting neurons whose somata reside in the injected hippocampus. That is, SP would no longer be able to activate NK1 receptors on bistratified and CCK-IR local circuit neurons, so compensatory mechanisms would either not be triggered or activated to a minimal extent. Therefore, in the contralateral side we have a more physiological-like activity, where all populations contacted by long-range interneurons are equally depressed.

This depression would translate into a disinhibition of the excitatory network, which in turn would lead to an increase of the ripple episodes, as explained above.

Analysing the various ripple parameters considered in this study, I observed no clear differences between control and SP treated recordings for neither of the parameters considered. This is likely because local SP injection activates diverse compensatory mechanisms in the injected hippocampus. Injection of SP in this regard seems to be perceived by the hippocampus as a weaker stimulus than Quinine, because in the Quinine experiments I was able to observe differences in the inter ripple intervals between control and drug injection state, where I was not able to observe any modifications following SP injection. On the other hand, it might be that interference (be it in a positive or negative direction) with the inhibitory network has little effect on length, amplitude and frequency (***Figs.16***, ***17*** and ***21***, respectively) of the ripple episodes. It therefore seems that interneurons modulate or influence these parameters to a minimal extent. Additionally, the observation that I.R.I. is not modified following SP injection (***Fig.17***) also points out that probably there is no modification in the ratio between theta and non-theta activity following SP injection.

In light of the information above, I confirmed that long projection neurons express NK1 receptors and are influenced by SP injection. Activation of NK1-R would lead to an increased excitability of the injected hippocampus, but other cell populations also affected by SP injection would contrast this excitability in the injected side. In addition, long projection neurons would also promote an increased excitation contralaterally, where they would increase the generation of ripple episodes presumably by acting on inhibitory neurons located in the CA3 area of the contralateral hippocampus.

Conclusions

In this study, I investigated the role of long projecting neurons in intra-hemispheric ripple synchronization. To test the idea that long-range interneurons would modify ripple activity in both sides of the hippocampus, I injected in one side of the brain drugs known to affect inhibitory activity. The only clear parameter that showed a marked modification following drugs injection was the number of ripples recorded. I also report a decrease in the inter ripple interval following gap-junction blockage. What seems to emerge from this study is that long projection neurons are involved in ripple synchronization, but this involvement is not as broad and powerful as it was expected. Indeed, almost all the parameters analysed showed no modification following Quinine and SP injection, testifying that the hippocampus has several feedback and feedforward mechanisms responsible for efficiently contrasting excessive activity from one group of cells, through the actions of one or several other groups of neurons. What is puzzling is the fact that, even though I observed no differences in most of the parameters recorded, I still observed a definite modification in the number of ripples recorded after drug injection. This observation seem to point out that inhibitory neurons and long range projecting interneurons might influence the generation of ripple episodes, which means that their connections with the CA3 area of each hippocampus might be more important than originally believed. In fact, interneurons whose somata reside in the CA1 would be in an ideal position to process information from that area of the hippocampus, and then transmit this information to the CA3 area through a feedback mechanism that propagates the information to both hippocampal hemispheres.

Taken together, my observations suggest that long-projecting inhibitory neurons actively participate in controlling ripple episodes synchronization in both sides of the hippocampus. This small population of neurons seems involved in influencing the number of ripple episodes, but not the parameters intrinsic to each episode (frequency, amplitude, length). In spite of their presumably low number, these neurons might play an important role in the neuronal

synchronization throughout the hippocampus and between the two hippocampi, possibly not limited to ripple oscillations. The proposed function of long-projection neurons is to modulate the global activity of the hippocampus, playing a role in intra-hippocampal as well as inter-hemispheric network synchronization, through a disinhibitory mechanism. Such a mechanism would work according to a master-slave model similar to the one reported in ***Fig.6***. Nonetheless, a new model is in order, which would focus more on the connections that long projecting interneurons have with CA3 interneurons, since this is where ripples are generated. This model is idealized in ***Fig.22*** for Quinine experiments and ***Fig.23*** for SP experiments.

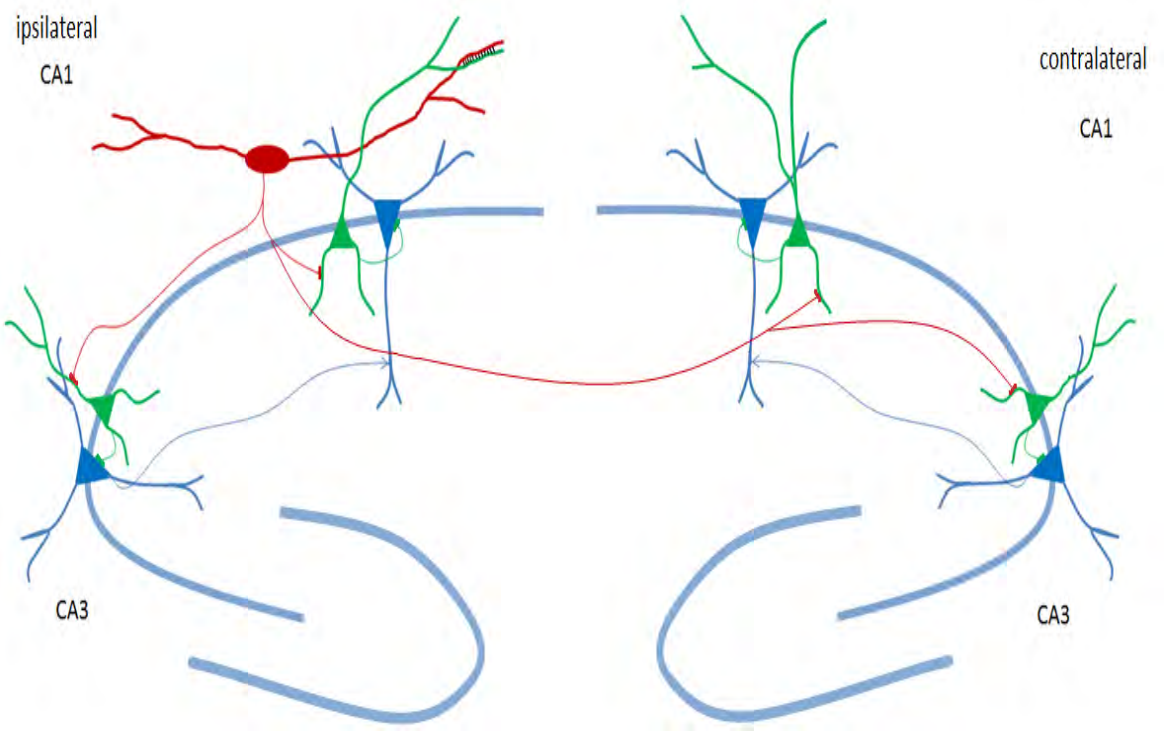

Fig.22. Idealized diagram of ripple generation, in presence of Quinine. Disruption of communications between local circuit interneurons (green triangles) and long projection neurons (red circle) through putative gap-junction blockage leads to an excessive inhibitory activity on pyramidal cells (blue triangles). The over-activation of the inhibitory network is carried to the contralateral hippocampus by *stratum oriens* long-projection neurons, with consequent decrease of generation of ripples in both hemispheres of the hippocampus. Thick lines represent dendritic arborisation, while thin lines represent axonal projections. Arrowheads represent excitatory synapses (Schaffer Collaterals), while dashes represent inhibitory synapses. Gap-junctions are represented by marks between the dendritic branches of the long projection neuron and the local circuit cell.

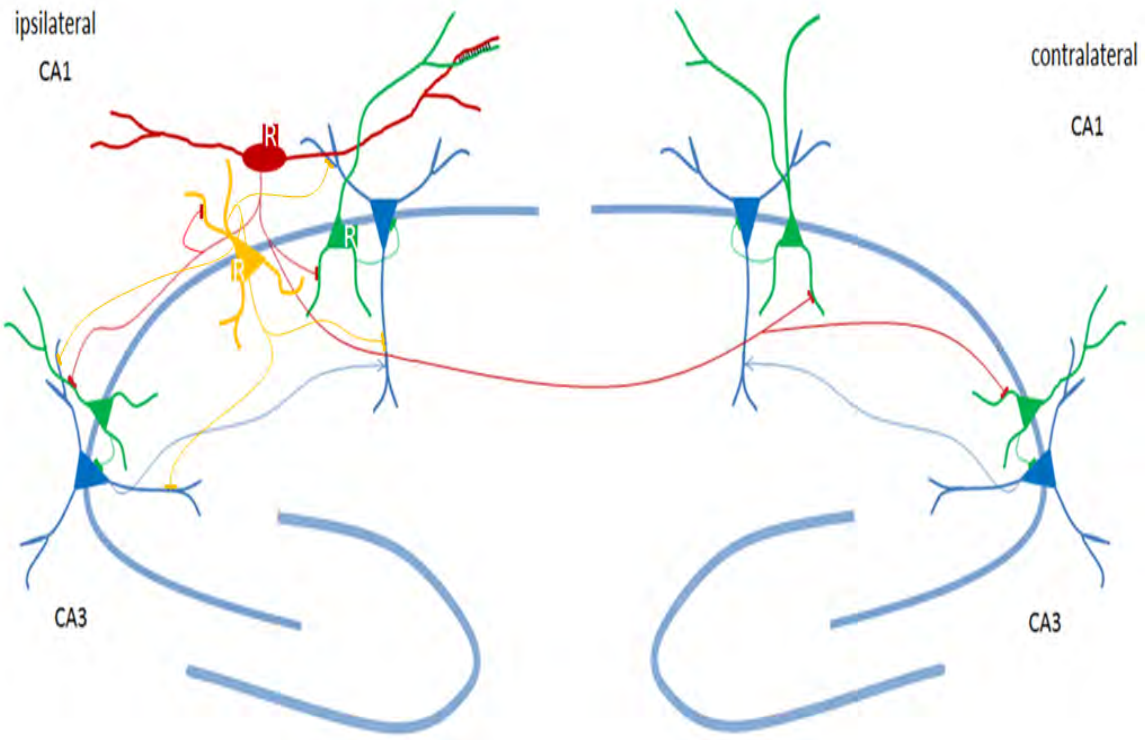

Fig.23. Idealized diagram of ripple generation, in presence of Substance P. Neurons expressing NK1 receptors (marked with an R in the diagram) promote a dual effect on pyramidal neurons (blue triangles). In the injected hippocampus, long projection neurons (red circle) would indirectly increase the excitatory drive of pyramidal cells, while local basket and bistratified neurons (green and yellow triangles, respectively) would directly increase the inhibitory drive on principal neurons. These two effects would compete for driving excitability on principal cells, with the resultant outcome of a minimal perturbation of ripple activity. In the contralateral side, inter-hemispheric projections by long-range neurons would instead be the only population to promote excitation of pyramidal cells, because SP does not activate contralateral basket and bistratified interneurons. This would lead to an increase in the excitatory drive of pyramidal neurons, causing an increase in ripple generation. Thick marks represent dendritic arborisation, while thin marks represent axonal projections. Arrowheads represent excitatory synapses (Schaffer Collaterals), while dashes represent inhibitory synapses. Gap-junctions are represented by marks between the dendritic branches of the long projection neuron and the local circuit cell.

In light of this information, I suggest that inhibitory cells located mainly in the CA1-CA3 *stratum oriens*, having both local and contralateral axonal arborisation, can in part explain the short latency between concomitantly occurring and highly synchronized ripple waves in both left and right hippocampi. Since ripple activity, along with its intra-hippocampal and inter-hemispheric synchronization is correlated to memory consolidation, the role of long-projection neurons might be of great importance for studies aimed to enhance the current knowledge of the hippocampus, particularly in relation to its importance in memory formation.

REFERENCES

1. Cajal, R.y., *Estructura del aste de Ammon y fascia dentate.* Ann Soc Esp Hist Nat, 1883. **22**.
2. Cajal, R.y., *Histologie du systeme nerveux de l'Homme et des Vertebres*1911, Paris: Maloine.
3. Nò, L.d., *Studies on the structure of the cerebral cortex. Continuation of the study of the ammonic system.* J. Psychol. Neurol., 1934. **46**: p. 113-177.
4. Engel, J., T.A. Pedley, and J. Aicardi, *Epilepsy : a comprehensive textbook*1998, Philadelphia: Lippincott-Raven.
5. Freund, T.F. and G. Buzsaki, *Interneurons of the hippocampus.* Hippocampus, 1996. **6**(4): p. 347-470.
6. Bland, S.K. and B.H. Bland, *Medial septal modulation of hippocampal theta cell discharges.* Brain Res, 1986. **375**(1): p. 102-16.
7. Ylinen, A., et al., *Sharp wave-associated high-frequency oscillation (200 Hz) in the intact hippocampus: network and intracellular mechanisms.* J Neurosci, 1995. **15**(1 Pt 1): p. 30-46.
8. Buzsaki, G., *Two-stage model of memory trace formation: a role for "noisy" brain states.* Neuroscience, 1989. **31**(3): p. 551-70.
9. Klausberger, T., et al., *Spike timing of dendrite-targeting bistratified cells during hippocampal network oscillations in vivo.* Nat Neurosci, 2004. **7**(1): p. 41-7.
10. Bland, B.H., *The physiology and pharmacology of hippocampal formation theta rhythms.* Prog Neurobiol, 1986. **26**(1): p. 1-54.
11. Deng, W., J.B. Aimone, and F.H. Gage, *New neurons and new memories: how does adult hippocampal neurogenesis affect learning and memory?* Nat Rev Neurosci, 2010. **11**(5): p. 339-50.
12. Buzsaki, G., *The hippocampo-neocortical dialogue.* Cereb Cortex, 1996. **6**(2): p. 81-92.
13. Leung, L.S., *Behavior-dependent evoked potentials in the hippocampal CA1 region of the rat. I. Correlation with behavior and EEG.* Brain Res, 1980. **198**(1): p. 95-117.
14. Csicsvari, J., et al., *Fast network oscillations in the hippocampal CA1 region of the behaving rat.* J Neurosci, 1999. **19**(16): p. RC20.
15. Kamondi, A., et al., *Theta oscillations in somata and dendrites of hippocampal pyramidal cells in vivo: activity-dependent phase-precession of action potentials.* Hippocampus, 1998. **8**(3): p. 244-61.
16. Kocsis, B., A. Bragin, and G. Buzsaki, *Interdependence of multiple theta generators in the hippocampus: a partial coherence analysis.* J Neurosci, 1999. **19**(14): p. 6200-12.
17. Vanderwolf, C.H., *Hippocampal electrical activity and voluntary movement in the rat.* Electroencephalogr Clin Neurophysiol, 1969. **26**(4): p. 407-18.
18. Chrobak, J.J. and G. Buzsaki, *Gamma oscillations in the entorhinal cortex of the freely behaving rat.* J Neurosci, 1998. **18**(1): p. 388-98.
19. Bragin, A., et al., *Gamma (40-100 Hz) oscillation in the hippocampus of the behaving rat.* J Neurosci, 1995. **15**(1 Pt 1): p. 47-60.
20. Buzsaki, G., L.W. Leung, and C.H. Vanderwolf, *Cellular bases of hippocampal EEG in the behaving rat.* Brain Res, 1983. **287**(2): p. 139-71.
21. Buzsaki, G., *Feed-forward inhibition in the hippocampal formation.* Prog Neurobiol, 1984. **22**(2): p. 131-53.
22. Freund, T.F. and M. Antal, *GABA-containing neurons in the septum control inhibitory interneurons in the hippocampus.* Nature, 1988. **336**(6195): p. 170-3.
23. Stewart, M. and S.E. Fox, *Do septal neurons pace the hippocampal theta rhythm?* Trends Neurosci, 1990. **13**(5): p. 163-8.
24. Buzsaki, G., et al., *High-frequency network oscillation in the hippocampus.* Science, 1992. **256**(5059): p. 1025-7.

25. Csicsvari, J., et al., *Oscillatory coupling of hippocampal pyramidal cells and interneurons in the behaving Rat.* J Neurosci, 1999. **19**(1): p. 274-87.
26. Hirase, H., et al., *Firing rates of hippocampal neurons are preserved during subsequent sleep episodes and modified by novel awake experience.* Proc Natl Acad Sci U S A, 2001. **98**(16): p. 9386-90.
27. Axmacher, N., et al., *Memory formation by neuronal synchronization.* Brain Res Rev, 2006. **52**(1): p. 170-82.
28. Lisman, J., *The theta/gamma discrete phase code occuring during the hippocampal phase precession may be a more general brain coding scheme.* Hippocampus, 2005. **15**(7): p. 913-22.
29. Chrobak, J.J. and G. Buzsaki, *Operational dynamics in the hippocampal-entorhinal axis.* Neurosci Biobehav Rev, 1998. **22**(2): p. 303-10.
30. Leung, L.S., *Generation of theta and gamma rhythms in the hippocampus.* Neurosci Biobehav Rev, 1998. **22**(2): p. 275-90.
31. Buzsaki, G., *Functions for interneuronal nets in the hippocampus.* Can J Physiol Pharmacol, 1997. **75**(5): p. 508-15.
32. Chrobak, J.J. and G. Buzsaki, *High-frequency oscillations in the output networks of the hippocampal-entorhinal axis of the freely behaving rat.* J Neurosci, 1996. **16**(9): p. 3056-66.
33. Wilson, M.A. and B.L. McNaughton, *Reactivation of hippocampal ensemble memories during sleep.* Science, 1994. **265**(5172): p. 676-9.
34. O'Neill, J., et al., *Reactivation of experience-dependent cell assembly patterns in the hippocampus.* Nat Neurosci, 2008. **11**(2): p. 209-15.
35. Buzsaki, G., *Theta rhythm of navigation: link between path integration and landmark navigation, episodic and semantic memory.* Hippocampus, 2005. **15**(7): p. 827-40.
36. Buzsaki, G., et al., *Hippocampal network patterns of activity in the mouse.* Neuroscience, 2003. **116**(1): p. 201-11.
37. Buzsaki, G., *Theta oscillations in the hippocampus.* Neuron, 2002. **33**(3): p. 325-40.
38. Klausberger, T., et al., *Complementary roles of cholecystokinin- and parvalbumin-expressing GABAergic neurons in hippocampal network oscillations.* J Neurosci, 2005. **25**(42): p. 9782-93.
39. Lee, M.G., et al., *Hippocampal theta activity following selective lesion of the septal cholinergic system.* Neuroscience, 1994. **62**(4): p. 1033-47.
40. Freeman, J.A. and C. Nicholson, *Experimental optimization of current source-density technique for anuran cerebellum.* J Neurophysiol, 1975. **38**(2): p. 369-82.
41. Mitzdorf, U., *Current source-density method and application in cat cerebral cortex: investigation of evoked potentials and EEG phenomena.* Physiol Rev, 1985. **65**(1): p. 37-100.
42. Kocsis, B., et al., *Separation of hippocampal theta dipoles by partial coherence analysis in the rat.* Brain Res, 1994. **660**(2): p. 341-5.
43. Kandel, E.R., J.H. Schwartz, and T.M. Jessell, *Principles of neural science*. 4th ed2000, New York: McGraw-Hill, Health Professions Division. xli, 1414 p.
44. Sik, A., et al., *Hippocampal CA1 interneurons: an in vivo intracellular labeling study.* J Neurosci, 1995. **15**(10): p. 6651-65.
45. Traub, R.D., et al., *Analysis of gamma rhythms in the rat hippocampus in vitro and in vivo.* J Physiol, 1996. **493 (Pt 2)**: p. 471-84.
46. Cobb, S.R., et al., *Synchronization of neuronal activity in hippocampus by individual GABAergic interneurons.* Nature, 1995. **378**(6552): p. 75-8.
47. Klausberger, T., et al., *Brain-state- and cell-type-specific firing of hippocampal interneurons in vivo.* Nature, 2003. **421**(6925): p. 844-8.
48. Jinno, S., et al., *Neuronal diversity in GABAergic long-range projections from the hippocampus.* J Neurosci, 2007. **27**(33): p. 8790-804.
49. Toth, K. and T.F. Freund, *Calbindin D28k-containing nonpyramidal cells in the rat hippocampus: their immunoreactivity for GABA and projection to the medial septum.* Neuroscience, 1992. **49**(4): p. 793-805.

50. Sik, A., et al., *Inhibitory CA1-CA3-hilar region feedback in the hippocampus.* Science, 1994. **265**(5179): p. 1722-4.
51. Gulyas, A.I., et al., *Interneurons are the local targets of hippocampal inhibitory cells which project to the medial septum.* Eur J Neurosci, 2003. **17**(9): p. 1861-72.
52. Shinohara, Y., et al., *Hippocampal CA3 and CA2 have distinct bilateral innervation patterns to CA1 in rodents.* Eur J Neurosci, 2012. **35**(5): p. 702-10.
53. Andersen, P., et al., *Functional characteristics of unmyelinated fibres in the hippocampal cortex.* Brain Res, 1978. **144**(1): p. 11-8.
54. Traub, R.D. and A. Bibbig, *A model of high-frequency ripples in the hippocampus based on synaptic coupling plus axon-axon gap junctions between pyramidal neurons.* J Neurosci, 2000. **20**(6): p. 2086-93.
55. Spruston, N., *Axonal gap junctions send ripples through the hippocampus.* Neuron, 2001. **31**(5): p. 669-71.
56. Maier, N., et al., *Reduction of high-frequency network oscillations (ripples) and pathological network discharges in hippocampal slices from connexin 36-deficient mice.* J Physiol, 2002. **541**(Pt 2): p. 521-8.
57. MacVicar, B.A. and F.E. Dudek, *Dye-coupling betwen CA3 pyramidal cells in slices of rat hippocampus.* Brain Res, 1980. **196**(2): p. 494-7.
58. MacVicar, B.A. and F.E. Dudek, *Electrotonic coupling between pyramidal cells: a direct demonstration in rat hippocampal slices.* Science, 1981. **213**(4509): p. 782-5.
59. Taylor, C.P. and F.E. Dudek, *A physiological test for electrotonic coupling between CA1 pyramidal cells in rat hippocampal slices.* Brain Res, 1982. **235**(2): p. 351-7.
60. Fisahn, A., et al., *Cholinergic induction of network oscillations at 40 Hz in the hippocampus in vitro.* Nature, 1998. **394**(6689): p. 186-9.
61. Singer, W. and C.M. Gray, *Visual feature integration and the temporal correlation hypothesis.* Annu Rev Neurosci, 1995. **18**: p. 555-86.
62. Steriade, M., et al., *Synchronization of fast (30-40 Hz) spontaneous oscillations in intrathalamic and thalamocortical networks.* J Neurosci, 1996. **16**(8): p. 2788-808.
63. Whittington, M.A., R.D. Traub, and J.G. Jefferys, *Synchronized oscillations in interneuron networks driven by metabotropic glutamate receptor activation.* Nature, 1995. **373**(6515): p. 612-5.
64. Draguhn, A., et al., *Electrical coupling underlies high-frequency oscillations in the hippocampus in vitro.* Nature, 1998. **394**(6689): p. 189-92.
65. Kosaka, T., *Gap junctions between non-pyramidal cell dendrites in the rat hippocampus (CA1 and CA3 regions).* Brain Res, 1983. **271**(1): p. 157-61.
66. Kosaka, T. and K. Hama, *Gap junctions between non-pyramidal cell dendrites in the rat hippocampus (CA1 and CA3 regions): a combined Golgi-electron microscopy study.* J Comp Neurol, 1985. **231**(2): p. 150-61.
67. Kita, H., T. Kosaka, and C.W. Heizmann, *Parvalbumin-immunoreactive neurons in the rat neostriatum: a light and electron microscopic study.* Brain Res, 1990. **536**(1-2): p. 1-15.
68. Condorelli, D.F., et al., *Expression of Cx36 in mammalian neurons.* Brain Res Brain Res Rev, 2000. **32**(1): p. 72-85.
69. Condorelli, D.F., et al., *Cloning of a new gap junction gene (Cx36) highly expressed in mammalian brain neurons.* Eur J Neurosci, 1998. **10**(3): p. 1202-8.
70. Venance, L., et al., *Connexin expression in electrically coupled postnatal rat brain neurons.* Proc Natl Acad Sci U S A, 2000. **97**(18): p. 10260-5.
71. Allen, K., et al., *Gap junctions between interneurons are required for normal spatial coding in the hippocampus and short-term spatial memory.* J Neurosci, 2011. **31**(17): p. 6542-52.
72. Buhl, D.L., et al., *Selective impairment of hippocampal gamma oscillations in connexin-36 knock-out mouse in vivo.* J Neurosci, 2003. **23**(3): p. 1013-8.

73. Hormuzdi, S.G., et al., *Impaired electrical signaling disrupts gamma frequency oscillations in connexin 36-deficient mice.* Neuron, 2001. **31**(3): p. 487-95.
74. Otsuka, M. and K. Yoshioka, *Neurotransmitter functions of mammalian tachykinins.* Physiol Rev, 1993. **73**(2): p. 229-308.
75. De Felipe, C., et al., *Altered nociception, analgesia and aggression in mice lacking the receptor for substance P.* Nature, 1998. **392**(6674): p. 394-7.
76. Bossaller, C., et al., *In vivo measurement of endothelium-dependent vasodilation with substance P in man.* Herz, 1992. **17**(5): p. 284-90.
77. Nakanishi, S., et al., *Molecular characterization of mammalian tachykinin receptors and a possible epithelial potassium channel.* Recent Prog Horm Res, 1990. **46**: p. 59-83; discussion 83-4.
78. Nagano, M., et al., *Distribution and pharmacological characterization of primate NK-1 and NK-3 tachykinin receptors in the central nervous system of the rhesus monkey.* Br J Pharmacol, 2006. **147**(3): p. 316-23.
79. Saffroy, M., et al., *Autoradiographic distribution of tachykinin NK2 binding sites in the rat brain: comparison with NK1 and NK3 binding sites.* Neuroscience, 2003. **116**(3): p. 761-73.
80. Humpel, C. and A. Saria, *Characterization of neurokinin binding sites in rat brain membranes using highly selective ligands.* Neuropeptides, 1993. **25**(1): p. 65-71.
81. Davies, S. and C. Kohler, *The substance P innervation of the rat hippocampal region.* Anat Embryol (Berl), 1985. **173**(1): p. 45-52.
82. Dodd, J. and J.S. Kelly, *The actions of cholecystokinin and related peptides on pyramidal neurones of the mammalian hippocampus.* Brain Res, 1981. **205**(2): p. 337-50.
83. Nakaya, Y., et al., *Immunohistochemical localization of substance P receptor in the central nervous system of the adult rat.* J Comp Neurol, 1994. **347**(2): p. 249-74.
84. Dreifuss, J.J. and M. Raggenbass, *Tachykinins and bombesin excite non-pyramidal neurones in rat hippocampus.* J Physiol, 1986. **379**: p. 417-28.
85. Kouznetsova, M. and A. Nistri, *Modulation by substance P of synaptic transmission in the mouse hippocampal slice.* Eur J Neurosci, 1998. **10**(10): p. 3076-84.
86. Kouznetsova, M. and A. Nistri, *Facilitation of cholinergic transmission by substance P methyl ester in the mouse hippocampal slice preparation.* Eur J Neurosci, 2000. **12**(2): p. 585-94.
87. McBain, C.J., T.J. DiChiara, and J.A. Kauer, *Activation of metabotropic glutamate receptors differentially affects two classes of hippocampal interneurons and potentiates excitatory synaptic transmission.* J Neurosci, 1994. **14**(7): p. 4433-45.
88. Agnati, L.F., et al., *Intercellular communication in the brain: wiring versus volume transmission.* Neuroscience, 1995. **69**(3): p. 711-26.
89. Huston, J.P. and R.U. Hasenohrl, *The role of neuropeptides in learning: focus on the neurokinin substance P.* Behav Brain Res, 1995. **66**(1-2): p. 117-27.
90. Sprick, U., et al., *Effects of chronic substance P treatment and intracranial fetal grafts on learning after hippocampal kainic acid lesions.* Peptides, 1996. **17**(2): p. 275-85.
91. Margineanu, D.G. and H. Klitgaard, *The connexin 36 blockers quinine, quinidine and mefloquine inhibit cortical spreading depression in a rat neocortical slice model in vitro.* Brain Res Bull, 2006. **71**(1-3): p. 23-8.
92. Srinivas, M., M.G. Hopperstad, and D.C. Spray, *Quinine blocks specific gap junction channel subtypes.* Proc Natl Acad Sci U S A, 2001. **98**(19): p. 10942-7.
93. Hasenohrl, R.U., et al., *Substance P and its role in neural mechanisms governing learning, anxiety and functional recovery.* Neuropeptides, 2000. **34**(5): p. 272-80.
94. Paxinos G., W.C., *The Rat Brain in Stereotaxic Coordinates*. 4th ed1998: Academic Press. 236.
95. Sullivan, D., et al., *Relationships between hippocampal sharp waves, ripples, and fast gamma oscillation: influence of dentate and entorhinal cortical activity.* J Neurosci, 2011. **31**(23): p. 8605-16.

96. O'Neill, J., T. Senior, and J. Csicsvari, *Place-selective firing of CA1 pyramidal cells during sharp wave/ripple network patterns in exploratory behavior.* Neuron, 2006. **49**(1): p. 143-55.
97. Schubert, T., et al., *Connexin36 mediates gap junctional coupling of alpha-ganglion cells in mouse retina.* J Comp Neurol, 2005. **485**(3): p. 191-201.
98. Parys, B., et al., *Intercellular calcium signaling between astrocytes and oligodendrocytes via gap junctions in culture.* Neuroscience, 2010. **167**(4): p. 1032-43.
99. Hajos, N., et al., *Cannabinoids inhibit hippocampal GABAergic transmission and network oscillations.* Eur J Neurosci, 2000. **12**(9): p. 3239-49.
100. Bragin, A., et al., *Hippocampal and entorhinal cortex high-frequency oscillations (100--500 Hz) in human epileptic brain and in kainic acid--treated rats with chronic seizures.* Epilepsia, 1999. **40**(2): p. 127-37.
101. Levesque, M., et al., *High-frequency (80-500 Hz) oscillations and epileptogenesis in temporal lobe epilepsy.* Neurobiol Dis, 2011. **42**(3): p. 231-41.
102. Staba, R.J., et al., *Quantitative analysis of high-frequency oscillations (80-500 Hz) recorded in human epileptic hippocampus and entorhinal cortex.* J Neurophysiol, 2002. **88**(4): p. 1743-52.
103. Bragin, A., et al., *High-frequency oscillations in human brain.* Hippocampus, 1999. **9**(2): p. 137-42.
104. Sik, A., M. Penttonen, and G. Buzsaki, *Interneurons in the hippocampal dentate gyrus: an in vivo intracellular study.* Eur J Neurosci, 1997. **9**(3): p. 573-88.
105. Hasenohrl, R.U., et al., *Chronic administration of neurokinin SP improves maze performance in aged Rattus norvegicus.* Behav Neural Biol, 1994. **62**(2): p. 110-20.
106. Hasenohrl, R.U., J.P. Huston, and T. Schuurman, *Neuropeptide substance P improves water maze performance in aged rats.* Psychopharmacology (Berl), 1990. **101**(1): p. 23-6.
107. Huston, J.P. and M.S. Oitzl, *The relationship between reinforcement and memory: parallels in the rewarding and mnemonic effects of the neuropeptide substance P.* Neurosci Biobehav Rev, 1989. **13**(2-3): p. 171-80.
108. Baude, A., et al., *Immunoreactivity for the GABAA receptor alpha1 subunit, somatostatin and Connexin36 distinguishes axoaxonic, basket, and bistratified interneurons of the rat hippocampus.* Cereb Cortex, 2007. **17**(9): p. 2094-107.
109. Gibson, J.R., M. Beierlein, and B.W. Connors, *Two networks of electrically coupled inhibitory neurons in neocortex.* Nature, 1999. **402**(6757): p. 75-9.
110. Szabadics, J., A. Lorincz, and G. Tamas, *Beta and gamma frequency synchronization by dendritic gabaergic synapses and gap junctions in a network of cortical interneurons.* J Neurosci, 2001. **21**(15): p. 5824-31.
111. Galarreta, M. and S. Hestrin, *A network of fast-spiking cells in the neocortex connected by electrical synapses.* Nature, 1999. **402**(6757): p. 72-5.
112. Zsiros, V. and G. Maccaferri, *Electrical coupling between interneurons with different excitable properties in the stratum lacunosum-moleculare of the juvenile CA1 rat hippocampus.* J Neurosci, 2005. **25**(38): p. 8686-95.
113. Price, C.J., et al., *Neurogliaform neurons form a novel inhibitory network in the hippocampal CA1 area.* J Neurosci, 2005. **25**(29): p. 6775-86.
114. Zhou, M., et al., *TWIK-1 and TREK-1 are potassium channels contributing significantly to astrocyte passive conductance in rat hippocampal slices.* J Neurosci, 2009. **29**(26): p. 8551-64.
115. Newman, E.A., D.A. Frambach, and L.L. Odette, *Control of extracellular potassium levels by retinal glial cell K+ siphoning.* Science, 1984. **225**(4667): p. 1174-5.
116. Orkand, R.K., J.G. Nicholls, and S.W. Kuffler, *Effect of nerve impulses on the membrane potential of glial cells in the central nervous system of amphibia.* J Neurophysiol, 1966. **29**(4): p. 788-806.
117. Cruikshank, S.J., et al., *Potent block of Cx36 and Cx50 gap junction channels by mefloquine.* Proc Natl Acad Sci U S A, 2004. **101**(33): p. 12364-9.
118. Girardeau, G., et al., *Selective suppression of hippocampal ripples impairs spatial memory.* Nat Neurosci, 2009. **12**(10): p. 1222-3.

119. Ego-Stengel, V. and M.A. Wilson, *Disruption of ripple-associated hippocampal activity during rest impairs spatial learning in the rat.* Hippocampus, 2010. **20**(1): p. 1-10.
120. Axmacher, N., C.E. Elger, and J. Fell, *Ripples in the medial temporal lobe are relevant for human memory consolidation.* Brain, 2008. **131**(Pt 7): p. 1806-17.
121. Mantyh, P.W., S.P. Hunt, and J.E. Maggio, *Substance P receptors: localization by light microscopic autoradiography in rat brain using [3H]SP as the radioligand.* Brain Res, 1984. **307**(1-2): p. 147-65.
122. Acsady, L., et al., *Immunostaining for substance P receptor labels GABAergic cells with distinct termination patterns in the hippocampus.* J Comp Neurol, 1997. **378**(3): p. 320-36.
123. Somogyi, P. and T. Klausberger, *Defined types of cortical interneurone structure space and spike timing in the hippocampus.* J Physiol, 2005. **562**(Pt 1): p. 9-26.

Acknowledgments

This was a long journey. I would never have been able to complete it without the constant support and patience of my supervisor, Attila Sík. Not only the best researcher I have had the honour to work with, but most importantly a great person. The best example a young researcher like me could one day aspire to be.

To my parents Antonio and Santina, because I know they are always there for me. To my brother Damian, for making me laugh every day.

E una dedica speciale a te, amica mia.

Ti voglio bene.